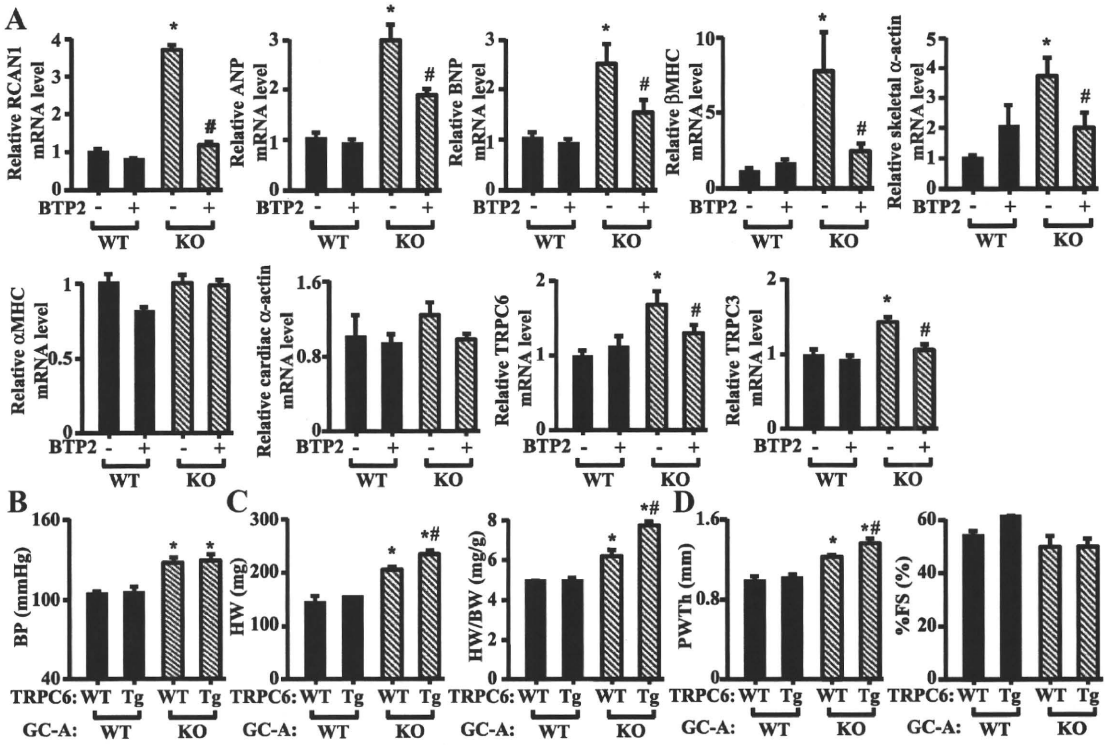

Figure 7. Inhibition of TRPC attenuates hypertrophic gene reprogramming in GC-A KO mice, whereas overexpression of TRPC6 exacerbated cardiac hypertrophy. A, Real-time RT-PCR analysis of relative expression of RCAN1, ANP, BNP, βMHC, skeletal α-actin, αMHC, cardiac α-actin, TRPC6, and TRPC3 mRNA in ventricular myocardium from 16-week-old WT and GC-A KO (KO) mice treated for 28 days with or without BTP2 (20 mg/g per day). Relative mRNA levels in WT without BTP2 were assigned a value of 1.0. Values are shown as means±SEM. *$P<0.05$ vs WT without BTP2; #$P<0.05$ vs KO without BTP2. **B and C,** Blood pressure (BP) **(B),** heart weight (HW) **(C, left)** and HW/BW ratios **(C, right)** in WT, TRPC6 Tg, GC-A KO, and TRPC6 Tg; GC-A KO mice. Values are shown as means±SEM. *$P<0.05$ vs WT; #$P<0.05$ vs GC-A KO. **D,** Echocardiographic parameters in WT, TRPC6 Tg GC-A KO, and TRPC6 Tg; GC-A KO mice. Graphs show posterior wall thickness (PWTh) (mm) and percentage fractional shortening (%FS). Values are shown as means±SEM. *$P<0.05$ vs WT; #$P<0.05$ vs GC-A KO.

Agonist-induced activation of the TRPC6 T69A mutant in the presence of ANP was around 80% to 90% of that seen with WT TRPC6 in the absence of ANP. Furthermore, even when we knocked down both RGS2 and RGS4, the significant inhibitory effect of ANP on agonist-induced Ca^{2+} influx was preserved in cardiac myocytes (Figure 5E through 5G; Online Figure IV, A and B). Thus, RGS-independent mechanisms also contribute to the antihypertrophic effects of cGMP-dependent signaling. This is not surprising, as multiple mechanisms would be expected to participate in the antihypertrophic effects exerted via the ANP/BNP-GC-A-cGMP-PKG pathway. In that regard, PKG also reportedly inhibits LTCC activity and calcineurin-NFAT signaling.[18] Although under our experimental conditions treatment with the LTCC blocker nifedipine did not significantly attenuate the inhibitory effect of ANP on agonist-induced Ca^{2+} influx into cardiac myocytes, inhibition of LTCCs can contribute to the antihypertrophic effects of ANP. Indeed, activation of TRPC3/6 has been shown to lead to LTCC activation,[24] and ANP may inhibit that activation, thereby inhibiting calcineurin-NFAT signaling. It therefore seems likely that ANP/BNP-GC-A-cGMP-PKG signaling inhibits prohypertrophic signaling pathways at multiple steps. ANP and BNP are already administered clinically to patients with acute heart failure.[46,47] But because, currently, these drugs are only administered intravenously, they are not available for use in the treatment of chronic pathological conditions such as cardiac hypertrophy and chronic heart failure. Development of nonpeptide GC-A agonists that can be administered orally may lead to the development of new therapeutic agents for preventing pathological cardiac hypertrophy and remodeling.

It has been shown in separate studies that GC-A is desensitized in failing human hearts[48] and that Ang II and ET-1 act to desensitize GC-A.[49] This makes it unlikely that under pathological conditions, endogenous cardiac ANP/BNP-GC-A-cGMP signaling would be sufficient to block the pathological signaling activity. Such disruption of the balance between anti- and prohypertrophic signaling would lead to further activation of TRPC3/6-dependent prohypertrophic signaling, thereby promoting the pathological cardiac remodeling. Thus inhibition of TRPC3/6 channel activity could be an effective therapeutic strategy for preventing cardiac remodeling under these pathological conditions. Indeed, our finding that BTP2 attenuated cardiac hypertrophy in GC-A KO and Ang II–infused mice may support this notion. In that regard, Pyr3 is a pyrazole compound recently identified as a specific inhibitor for TRPC3 that blocks Ca^{2+} influx carried by TRPC3/6 heteromeric complexes and by TRPC3 homomeric complexes. Moreover, Pyr3 also inhibited Ang II–induced hypertrophic responses in cultured cardiac myocytes more

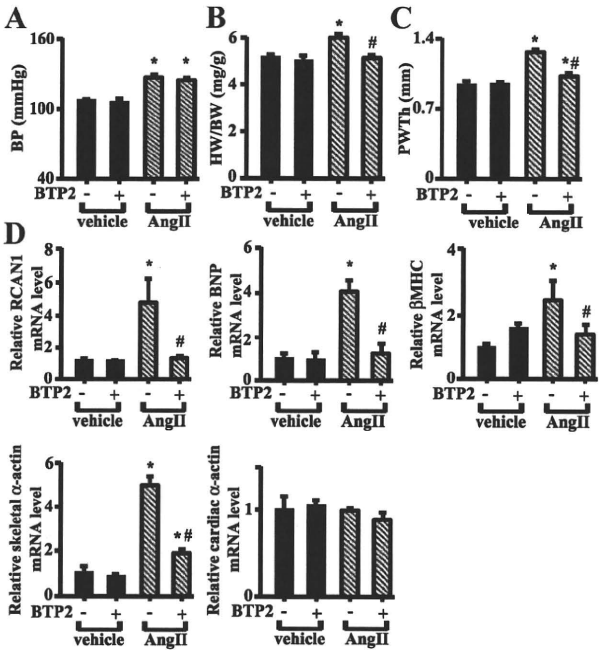

Figure 8. Inhibition of TRPC attenuates angiotensin II-induced cardiac hypertrophy in mice. A, Blood pressure (BP) in mice treated with or without Ang II (0.6 mg/kg per day) and/or BTP2 (20 mg/g per day). Values are shown as means±SEM. *$P<0.05$ vs control. **B,** HW/BW ratio (mg/g) in mice treated with or without Ang II (0.6 mg/kg per day) and BTP2 (20 mg/g per day). Values are shown as means±SEM. *$P<0.05$ vs control; #$P<0.05$ vs mice treated with Ang II and without BTP2. **C,** Posterior wall thickness (PWTh) (mm) evaluated by echocardiography in mice treated with of without Ang II (0.6 mg/kg per day) and BTP2 (20 mg/g per day). Values are shown as means±SEM. *$P<0.05$ vs control; #$P<0.05$ vs mice treated with Ang II and without BTP2. **D,** Real-time RT-PCR analysis of relative expression of RCAN1, BNP, βMHC, skeletal α-actin, and cardiac α-actin mRNA in ventricular myocardium from 10-week-old mice treated for 14 days with or without Ang II (0.6 mg/kg per day) and/or BTP2 (20 mg/g per day). Relative mRNA levels in control mice without Ang II and BTP2 were assigned a value of 1.0. Values are shown as means±SEM. *$P<0.05$ vs control; #$P<0.05$ vs mice treated with Ang II and without BTP2.

potently than BTP2.[37] In our study, knocking down either TRPC3 or -6 in cardiac myocytes significantly inhibited ET-1– and Ang II–induced increases in Ca^{2+} oscillation to levels comparable to those seen when both TRPC3 and -6 were knocked down simultaneously (Online Figure II, A through J). This raises the possibility that a TRPC3/6 heteromeric complex plays a key role in mediating agonist-induced prohypertrophic signaling in cardiac myocytes. Development of highly specific TRPC6 inhibitors could lead to the development of more potent and safer agents with which to prevent pathological cardiac remodeling and heart failure.

Acknowledgments

We thank Yukari Kubo for excellent secretarial work. We also thank E. N. Olson for providing us TRPC6 Tg mice.

Sources of Funding

This research was supported by Grants-in-Aid for Scientific Research from the Japan Society for the Promotion of Science (to K.K., H. Kinoshita and K.N.); a grant from the Japanese Ministry of Health, Labour and Welfare (to K.N.); grants from the Mitsubishi Foundation, the Mochida Memorial Foundation for Medical and Pharmaceutical Research, the Uehara Memorial Foundation, the Japan Heart Foundation/Novartis Grant for Research Award on Molecular and Cellular Cardiology, the Japan Foundation for Applied Enzymology, the Mitsubishi Pharma Research Foundation, the Astellas Foundation for Research on Metabolic Disorders, the Kanae Foundation for the Promotion of Medical Science, the Ichiro Kanehara Foundation, the Suzuken Memorial Foundation, the Vehicle Racing Commemorative Foundation, the Japan Research Promotion Society for Cardiovascular diseases, the Takeda Medical Research Foundation, the Hohansha Foundation (to K.K.), and the Kimura Memorial Heart Foundation (to H. Kinoshita).

Disclosures

None.

References

1. Molkentin JD. Calcineurin-NFAT signaling regulates the cardiac hypertrophic response in coordination with the MAPKs. *Cardiovasc Res.* 2004; 63:467–475.
2. Bubikat A, De Windt LJ, Zetsche B, Fabritz L, Sickler H, Eckardt D, Godecke A, Baba HA, Kuhn M. Local atrial natriuretic peptide signaling prevents hypertensive cardiac hypertrophy in endothelial nitric-oxide synthase-deficient mice. *J Biol Chem.* 2005;280: 21594–21599.
3. de Bold AJ, Borenstein HB, Veress AT, Sonnenberg H. A rapid and potent natriuretic response to intravenous injection of atrial myocardial extract in rats. *Life Sci.* 1981;28:89–94.
4. Ogawa Y, Itoh H, Nakao K. Molecular biology and biochemistry of natriuretic peptide family. *Clin Exp Pharmacol Physiol.* 1995;22: 49–53.
5. McGrath MF, de Bold ML, de Bold AJ. The endocrine function of the heart. *Trends Endocrinol Metab.* 2005;16:469–477.
6. Chinkers M, Garbers DL, Chang MS, Lowe DG, Chin HM, Goeddel DV, Schulz S. A membrane form of guanylate cyclase is an atrial natriuretic peptide receptor. *Nature.* 1989;338:78–83.
7. Mukoyama M, Nakao K, Hosoda K, Suga S, Saito Y, Ogawa Y, Shirakami G, Jougasaki M, Obata K, Yasue H, Kambayashi Y, Inouye K, Imura H. Brain natriuretic peptide as a novel cardiac hormone in humans. Evidence for an exquisite dual natriuretic peptide system, atrial natriuretic peptide and brain natriuretic peptide. *J Clin Invest.* 1991;87:1402–1412.
8. Saito Y, Nakao K, Arai H, Nishimura K, Okumura K, Obata K, Takemura G, Fujiwara H, Sugawara A, Yamada T, Itoh H, Mukoyama M, Hosoda K, Kawai C, Ban T, Yasue H, Imura H. Augmented expression of atrial natriuretic polypeptide gene in ventricle of human failing heart. *J Clin Invest.* 1989;83:298–305.
9. Tamura N, Ogawa Y, Chusho H, Nakamura K, Nakao K, Suda M, Kasahara M, Hashimoto R, Katsuura G, Mukoyama M, Itoh H, Saito Y, Tanaka I, Otani H, Katsuki M. Cardiac fibrosis in mice lacking brain natriuretic peptide. *Proc Natl Acad Sci U S A.* 2000;97: 4239–4244.
10. Calderone A, Thaik CM, Takahashi N, Chang DL, Colucci WS. Nitric oxide, atrial natriuretic peptide, and cyclic GMP inhibit the growth-promoting effects of norepinephrine in cardiac myocytes and fibroblasts. *J Clin Invest.* 1998;101:812–818.
11. Kishimoto I, Rossi K, Garbers DL. A genetic model provides evidence that the receptor for atrial natriuretic peptide (guanylyl cyclase-A) inhibits cardiac ventricular myocyte hypertrophy. *Proc Natl Acad Sci U S A.* 2001;98:2703–2706.
12. Knowles JW, Esposito G, Mao L, Hagaman JR, Fox JE, Smithies O, Rockman HA, Maeda N. Pressure-independent enhancement of cardiac hypertrophy in natriuretic peptide receptor A-deficient mice. *J Clin Invest.* 2001;107:975–984.
13. Holtwick R, van Eickels M, Skryabin BV, Baba HA, Bubikat A, Begrow F, Schneider MD, Garbers DL, Kuhn M. Pressure-independent cardiac hypertrophy in mice with cardiomyocyte-restricted inactivation of the atrial natriuretic peptide receptor guanylyl cyclase-A. *J Clin Invest.* 2003; 111:1399–1407.

14. Saito Y, Nakao K, Nishimura K, Sugawara A, Okumura K, Obata K, Sonoda R, Ban T, Yasue H, Imura H. Clinical application of atrial natriuretic polypeptide in patients with congestive heart failure: beneficial effects on left ventricular function. *Circulation*. 1987;76: 115–124.
15. Tokudome T, Horio T, Kishimoto I, Soeki T, Mori K, Kawano Y, Kohno M, Garbers DL, Nakao K, Kangawa K. Calcineurin-nuclear factor of activated T cells pathway-dependent cardiac remodeling in mice deficient in guanylyl cyclase A, a receptor for atrial and brain natriuretic peptides. *Circulation*. 2005;111:3095–3104.
16. Takahashi N, Saito Y, Kuwahara K, Harada M, Kishimoto I, Ogawa Y, Kawakami R, Nakagawa Y, Nakanishi M, Nakao K. Angiotensin II-induced ventricular hypertrophy and extracellular signal-regulated kinase activation are suppressed in mice overexpressing brain natriuretic peptide in circulation. *Hypertens Res*. 2003;26:847–853.
17. Kilic A, Velic A, De Windt LJ, Fabritz L, Voss M, Mitko D, Zwiener M, Baba HA, van Eickels M, Schlatter E, Kuhn M. Enhanced activity of the myocardial Na+/H+ exchanger NHE-1 contributes to cardiac remodeling in atrial natriuretic peptide receptor-deficient mice. *Circulation*. 2005;112:2307–2317.
18. Fiedler B, Lohmann SM, Smolenski A, Linnemuller S, Pieske B, Schroder F, Molkentin JD, Drexler H, Wollert KC. Inhibition of calcineurin-NFAT hypertrophy signaling by cGMP-dependent protein kinase type I in cardiac myocytes. *Proc Natl Acad Sci U S A*. 2002;99: 11363–11368.
19. Pedram A, Razandi M, Kehrl J, Levin ER. Natriuretic peptides inhibit G protein activation. Mediation through cross-talk between cyclic GMP-dependent protein kinase and regulators of G protein-signaling proteins. *J Biol Chem*. 2000;275:7365–7372.
20. Tokudome T, Kishimoto I, Horio T, Arai Y, Schwenke DO, Hino J, Okano I, Kawano Y, Kohno M, Miyazato M, Nakao K, Kangawa K. Regulator of G-protein signaling subtype 4 mediates antihypertrophic effect of locally secreted natriuretic peptides in the heart. *Circulation*. 2008;117:2329–2339.
21. Molkentin JD, Lu JR, Antos CL, Markham B, Richardson J, Robbins J, Grant SR, Olson EN. A calcineurin-dependent transcriptional pathway for cardiac hypertrophy. *Cell*. 1998;93:215–228.
22. Nakayama H, Wilkin BJ, Bodi I, Molkentin JD. Calcineurin-dependent cardiomyopathy is activated by TRPC in the adult mouse heart. *FASEB J*. 2006;20:1660–1670.
23. Kuwahara K, Wang Y, McAnally J, Richardson JA, Bassel-Duby R, Hill JA, Olson EN. TRPC6 fulfills a calcineurin signaling circuit during pathologic cardiac remodeling. *J Clin Invest*. 2006;116:3114–3126.
24. Onohara N, Nishida M, Inoue R, Kobayashi H, Sumimoto H, Sato Y, Mori Y, Nagao T, Kurose H. TRPC3 and TRPC6 are essential for angiotensin II-induced cardiac hypertrophy. *EMBO J*. 2006;25: 5305–5316.
25. Montell C. The TRP superfamily of cation channels. *Sci STKE*. 2005; 2005:re3.
26. Nishida M, Kurose H. Roles of TRP channels in the development of cardiac hypertrophy. *Naunyn Schmiedebergs Arch Pharmacol*. 2008;378: 395–406.
27. Kwan HY, Huang Y, Yao X. Regulation of canonical transient receptor potential isoform 3 (TRPC3) channel by protein kinase G. *Proc Natl Acad Sci U S A*. 2004;101:2625–2630.
28. Takahashi S, Lin H, Geshi N, Mori Y, Kawarabayashi Y, Takami N, Mori MX, Honda A, Inoue R. Nitric oxide-cGMP-protein kinase G pathway negatively regulates vascular transient receptor potential channel TRPC6. *J Physiol*. 2008;586:4209–4223.
29. Yang J, Rothermel B, Vega RB, Frey N, McKinsey TA, Olson EN, Bassel-Duby R, Williams RS. Independent signals control expression of the calcineurin inhibitory proteins MCIP1 and MCIP2 in striated muscles. *Circ Res*. 2000;87:e61–e68.
30. Kuwahara K, Saito Y, Ogawa E, Takahashi N, Nakagawa Y, Naruse Y, Harada M, Hamanaka I, Izumi T, Miyamoto Y, Kishimoto I, Kawakami R, Nakanishi M, Mori N, Nakao K. The neuron-restrictive silencer element-neuron-restrictive silencer factor system regulates basal and endothelin 1-inducible atrial natriuretic peptide gene expression in ventricular myocytes. *Mol Cell Biol*. 2001;21:2085–2097.
31. Shi J, Takahashi S, Jin XH, Li YQ, Ito Y, Mori Y, Inoue R. Myosin light chain kinase-independent inhibition by ML-9 of murine TRPC6 channels expressed in HEK293 cells. *Br J Pharmacol*. 2007;152:122–131.
32. Kinoshita H, Kuwahara K, Takano M, Arai Y, Kuwabara Y, Yasuno S, Nakagawa Y, Nakanishi M, Harada M, Fujiwara M, Murakami M, Ueshima K, Nakao K. T-type Ca2+ channel blockade prevents sudden death in mice with heart failure. *Circulation*. 2009;120:743–752.
33. Adachi Y, Saito Y, Kishimoto I, Harada M, Kuwahara K, Takahashi N, Kawakami R, Nakanishi M, Nakagawa Y, Tanimoto K, Saitoh Y, Yasuno S, Usami S, Iwai M, Horiuchi M, Nakao K. Angiotensin II type 2 receptor deficiency exacerbates heart failure and reduces survival after acute myocardial infarction in mice. *Circulation*. 2003; 107:2406–2408.
34. Kuwahara K, Saito Y, Takano M, Arai Y, Yasuno S, Nakagawa Y, Takahashi N, Adachi Y, Takemura G, Horie M, Miyamoto Y, Morisaki T, Kuratomi S, Noma A, Fujiwara H, Yoshimasa Y, Kinoshita H, Kawakami R, Kishimoto I, Nakanishi M, Usami S, Saito Y, Harada M, Nakao K. NRSF regulates the fetal cardiac gene program and maintains normal cardiac structure and function. *EMBO J*. 2003;22:6310–6321.
35. Bush EW, Hood DB, Papst PJ, Chapo JA, Minobe W, Bristow MR, Olson EN, McKinsey TA. Canonical transient receptor potential channels promote cardiomyocyte hypertrophy through activation of calcineurin signaling. *J Biol Chem*. 2006;281:33487–33496.
36. He LP, Hewavitharana T, Soboloff J, Spassova MA, Gill DL. A functional link between store-operated and TRPC channels revealed by the 3,5-bis(trifluoromethyl)pyrazole derivative, BTP2. *J Biol Chem*. 2005; 280:10997–11006.
37. Kiyonaka S, Kato K, Nishida M, Mio K, Numaga T, Sawaguchi Y, Yoshida T, Wakamori M, Mori E, Numata T, Ishii M, Takemoto H, Ojida A, Watanabe K, Uemura A, Kurose H, Morii T, Kobayashi T, Sato Y, Sato C, Hamachi I, Mori Y. Selective and direct inhibition of TRPC3 channels underlies biological activities of a pyrazole compound. *Proc Natl Acad Sci U S A*. 2009;106:5400–5405.
38. Yonetoku Y, Kubota H, Okamoto Y, Ishikawa J, Takeuchi M, Ohta M, Tsukamoto S. Novel potent and selective calcium-release-activated calcium (CRAC) channel inhibitors. Part 2: Synthesis and inhibitory activity of aryl-3-trifluoromethylpyrazoles. *Bioorg Med Chem*. 2006;14: 5370–5383.
39. Zitt C, Strauss B, Schwarz EC, Spaeth N, Rast G, Hatzelmann A, Hoth M. Potent inhibition of Ca2+ release-activated Ca2+ channels and T-lymphocyte activation by the pyrazole derivative BTP2. *J Biol Chem*. 2004;279:12427–12437.
40. Ishikawa J, Ohga K, Yoshino T, Takezawa R, Ichikawa A, Kubota H, Yamada T. A pyrazole derivative, YM-58483, potently inhibits store-operated sustained Ca2+ influx and IL-2 production in T lymphocytes. *J Immunol*. 2003;170:4441–4449.
41. Takimoto E, Koitabashi N, Hsu S, Ketner EA, Zhang M, Nagayama T, Bedja D, Gabrielson KL, Blanton R, Siderovski DP, Mendelsohn ME, Kass DA. Regulator of G protein signaling 2 mediates cardiac compensation to pressure overload and antihypertrophic effects of PDE5 inhibition in mice. *J Clin Invest*. 2009;119:408–420.
42. Tang KM, Wang GR, Lu P, Karas RH, Aronovitz M, Heximer SP, Kaltenbronn KM, Blumer KJ, Siderovski DP, Zhu Y, Mendelsohn ME. Regulator of G-protein signaling-2 mediates vascular smooth muscle relaxation and blood pressure. *Nat Med*. 2003;9:1506–1512.
43. Lopez MJ, Wong SK, Kishimoto I, Dubois S, Mach V, Friesen J, Garbers DL, Beuve A. Salt-resistant hypertension in mice lacking the guanylyl cyclase-A receptor for atrial natriuretic peptide. *Nature*. 1995;378:65–68.
44. Li Y, Kishimoto I, Saito Y, Harada M, Kuwahara K, Izumi T, Takahashi N, Kawakami R, Tanimoto K, Nakagawa Y, Nakanishi M, Adachi Y, Garbers DL, Fukamizu A, Nakao K. Guanylyl cyclase-A inhibits angiotensin II type 1A receptor-mediated cardiac remodeling, an endogenous protective mechanism in the heart. *Circulation*. 2002; 106:1722–1728.
45. Kishimoto I, Dubois SK, Garbers DL. The heart communicates with the kidney exclusively through the guanylyl cyclase-A receptor: acute handling of sodium and water in response to volume expansion. *Proc Natl Acad Sci U S A*. 1996;93:6215–6219.
46. Colucci WS, Elkayam U, Horton DP, Abraham WT, Bourge RC, Johnson AD, Wagoner LE, Givertz MM, Liang CS, Neibaur M, Haught WH, LeJemtel TH. Intravenous nesiritide, a natriuretic peptide, in the treatment of decompensated congestive heart failure. Nesiritide Study Group. *N Engl J Med*. 2000;343:246–253.

47. Yoshimura M, Yasue H, Ogawa H. Pathophysiological significance and clinical application of ANP and BNP in patients with heart failure. *Can J Physiol Pharmacol.* 2001;79:730–735.
48. Tsutamoto T, Kanamori T, Morigami N, Sugimoto Y, Yamaoka O, Kinoshita M. Possibility of downregulation of atrial natriuretic peptide receptor coupled to guanylate cyclase in peripheral vascular beds of patients with chronic severe heart failure. *Circulation.* 1993;87:70–75.
49. Potter LR, Abbey-Hosch S, Dickey DM. Natriuretic peptides, their receptors, and cyclic guanosine monophosphate-dependent signaling functions. *Endocr Rev.* 2006;27:47–72.

Novelty and Significance

What Is Known?

- Under pathological conditions, the ventricular expression of 2 peptide mediators, atrial natriuretic peptide (ANP) and brain natriuretic peptide (BNP), is increased in the heart. These peptides act as both endocrine and local antihypertrophic factors. However, the molecular mechanisms by which ANP/BNP inhibit cardiac hypertrophy remain unclear.
- Transient receptor potential subfamily C (TRPC)3 and -6 form homo- and heteromultimeric cation channels that are activated directly by diacylglycerol following receptor activation and reportedly serve as positive upstream regulators of the pathological calcineurin-NFAT signaling pathway in cardiac myocytes.

What New Information Does This Article Contribute?

- We demonstrate that ANP/BNP acts via the guanylyl cyclase (GC)-A-cGMP-protein kinase (PK)G pathway to inhibit TRPC6 channel activity, which in turn suppresses the subsequent activation of the prohypertrophic calcineurin-nuclear factor of activated T cells (NFAT) signaling pathway.
- The present study suggests that inhibition of TRPC6 could be an effective therapeutic strategy for preventing pathological cardiac hypertrophy and remodeling.

Characterization of the crosstalk among the cardiac signaling pathways that promote or antagonize cardiac hypertrophy should lead to a better understanding of molecular processes underlying the development of heart failure and ultimately to the discovery of novel therapeutic approaches for preventing pathological cardiac remodeling and heart failure. The cardiac hormones ANP and BNP reportedly exert antihypertrophic effects on the heart via their common receptor, GC-A, which catalyzes the synthesis of cGMP, leading to activation of PKG. Details of molecular mechanisms via which ANP/BNP-GC-A signaling inhibit cardiac hypertrophy are not well understood. The present study demonstrates that ANP/BNP-GC-A-cGMP-PKG signaling pathway inhibits TRPC6 activity by phosphorylation of threonine 69, which in turn suppresses prohypertrophic calcineurin-NFAT signaling. In mice lacking GC-A, BTP2, a selective TRPC channel blocker, significantly attenuated the cardiac hypertrophy otherwise seen. Conversely, overexpression of TRPC6 in mice lacking GC-A exacerbated cardiac hypertrophy. BTP2 also significantly inhibited angiotensin II-induced cardiac hypertrophy in mice. The present study reports the novel finding that inhibition of TRPC6 contributes to the antihypertrophic effects exerted by ANP/BNP-GC-A-cGMP-PKG signaling. These results suggest that inhibition of TRPC6 could be an effective therapeutic strategy for preventing pathological cardiac hypertrophy.

Circulating C-Type Natriuretic Peptide (CNP) Rescues Chondrodysplastic CNP Knockout Mice from Their Impaired Skeletal Growth and Early Death

Toshihito Fujii, Yasato Komatsu, Akihiro Yasoda, Eri Kondo, Tetsuro Yoshioka, Takuo Nambu, Naotestu Kanamoto, Masako Miura, Naohisa Tamura, Hiroshi Arai, Masashi Mukoyama, and Kazuwa Nakao

Department of Medicine and Clinical Science, Kyoto University Graduate School of Medicine, Kyoto 606-8507, Japan

C-type natriuretic peptide (CNP) is a potent stimulator of endochondral bone growth through a subtype of membranous guanylyl cyclase receptor, GC-B. Although its two cognate natriuretic peptides, ANP and BNP, are cardiac hormones produced from heart, CNP is thought to act as an autocrine/paracrine regulator. To elucidate whether systemic administration of CNP would be a novel medical treatment for chondrodysplasias, for which no drug therapy has yet been developed, we investigated the effect of circulating CNP by using the CNP transgenic mice with an increased circulating CNP under the control of human serum amyloid P component promoter (*SAP-Nppc-Tg* mice). *SAP-Nppc-Tg* mice developed prominent overgrowth of bones formed through endochondral ossification. In organ culture experiments, the growth of tibial explants of *SAP-Nppc-Tg* mice was not changed from that of their wild-type littermates, exhibiting that the stimulatory effect on endochondral bone growth observed in *SAP-Nppc-Tg* mice is humoral. Then we crossed chondrodysplastic CNP-depleted mice with *SAP-Nppc-Tg* mice. Impaired endochondral bone growth in CNP knockout mice were considerably and significantly recovered by increased circulating CNP, followed by the improvement in not only their longitudinal growth but also their body weight. In addition, the mortality of CNP knockout mice was greatly decreased by circulating CNP. Systemic administration of CNP might have therapeutic potential against not only impaired skeletal growth but also other aspects of impaired growth including impaired body weight gain in patients suffering from chondrodysplasias and might resultantly protect them from their early death. (***Endocrinology* 151: 4381–4388, 2010**)

Recent studies have elucidated that C-type natriuretic peptide (CNP) is a crucial regulator of endochondral bone growth (1, 2). The biological actions of CNP are thought to be mediated by the production of intracellular second-messenger cGMP through a subtype of membranous guanylyl cyclase receptor, guanylyl cyclase (GC)-B (3). We have exhibited that both CNP and GC-B are expressed in the proliferative and prehypertrophic chondrocyte layers of the growth plate (1) and that CNP or GC-B knockout mice develop severely short stature phenotype owing to their impaired endochondral bone growth (1, 4). On the contrary, mice with targeted overexpression of CNP in the growth plate by using type II collagen promoter exhibit prominent skeletal overgrowth (5, 6).

After these discoveries, we planned to translate this strong stimulatory effect of the CNP/GC-B system on bone growth into clinical treatment for patients suffering from diseases with impaired skeletal growth. Chondrodysplasias are a group of genetic disorders characterized by impaired skeletal growth. The many different forms of chondrodysplasias add to produce a significant number of affected individuals with significant morbidity and mortality (7). Nevertheless, no efficient drug therapy has been developed to date for the treatment of chondrodysplasias.

ISSN Print 0013-7227 ISSN Online 1945-7170
Printed in U.S.A.

doi: 10.1210/en.2010-0078 Received January 20, 2010. Accepted June 3, 2010.
First Published Online July 7, 2010

Abbreviations: CNP, C-type natriuretic peptide; DIG, digoxigenin; GC, guanylyl cyclase; HE, hematoxylin and eosin; PCNA, proliferating cell nuclear antigen; SAP, serum amyloid P.

In our previous report, we achieved targeted overexpression of CNP in the growth plate of a mice model of achondroplasia (8), the most common form of chondrodysplasias with a constitutive active mutation in the fibroblast growth factor receptor 3 gene (9), and successfully treated its impaired skeletal growth and short stature phenotype (5).

In contrast to atrial natriuretic peptide and brain natriuretic peptide, the two cognate natriuretic peptides of CNP that act as cardiac hormones produced predominantly from atrium and ventricle of heart, respectively (10, 11), CNP is thought to be an autocrine/paracrine regulator, rather than an endocrine regulator (12, 13). Because we have to evaluate the effect of circulating CNP on endochondral bone growth in case we use CNP as a drug for chondrodysplasias via systemic administration, we generated CNP transgenic mice with increased circulating CNP as a model of systemic administration of CNP (14): these transgenic mice carried the human serum amyloid P (SAP) component promoter/mouse CNP fusion gene (*SAP-Nppc-Tg*), and the expression of the transgene was targeted to the liver (15). *SAP-Nppc-Tg* mice exhibited prominent overgrowth of bones formed through endochondral ossification (14), and furthermore, we successfully rescued achondroplastic model mice from their impaired bone growth by crossing them with *SAP-Nppc-Tg* mice (16).

In the present study, we further investigated the effect of circulating CNP by using *SAP-Nppc-Tg* mice. At first, to certify the humoral effect of the overexpressed CNP in *SAP-Nppc-Tg* mice on endochondral bone growth, we performed organ culture experiments by using tibial explants from *SAP-Nppc-Tg* mice and compared them with those from cartilage-targeted CNP transgenic mice under the control of type II collagen promoter (*Col2-Nppc-Tg* mice) (5). Then we studied the effects of circulating CNP on the chondrodysplastic CNP knockout ($Nppc^{-/-}$) mice by crossing them with *SAP-Nppc-Tg* mice.

Materials and Methods

Animals

Generation of CNP transgenic mice under the control of human SAP component promoter (*SAP-Nppc-Tg* mice) was reported previously (14). These mice carried the human SAP/mouse CNP fusion gene, and CNP overexpression in these mice was targeted to the liver (15). *SAP-Nppc-Tg* mice were intended to have increased circulating CNP levels, and plasma CNP concentrations measured by RIA were 84% higher in *SAP-Nppc-Tg* mice than in wild-type mice (14). Generation of CNP transgenic mice under the control of mouse type II collagen promoter (*Col2-Nppc-Tg* mice) (5) and CNP knockout mice ($Nppc^{-/-}$ mice) (1) was also described previously.

To generate $Nppc^{-/-}$ mice carrying *SAP-Nppc* transgene, male $Nppc^{+/-}$ mice were mated with female *SAP-Nppc-Tg* mice, and female F1 offspring heterozygous for both the transgene and the *Nppc* allele ablation were mated with male F1 offspring heterozygous only for the *Nppc* allele ablation to generate $Nppc^{-/-}$ mice with the transgene expression ($Nppc^{-/-}$/*SAP-Nppc-Tg* mice). For generation of homozygous *SAP-Nppc-Tg* mice, male and female heterozygous *SAP-Nppc-Tg* mice were mated, and the genotype of the resultant transgenic mice was determined by quantifying *SAP-Nppc* transgene using StepOnePlus real-time PCR systems (Applied Biosystems Inc., Foster City, CA).

The care of the animals and all experiments were conducted in accordance with the institutional guidelines of Kyoto University Graduate School of Medicine.

Organ culture

Tibias from fetal *SAP-Nppc-Tg* mice and their wild-type littermates (on d 16 of pregnancy), newborn *Col2-Nppc-Tg* mice and their wild-type littermates, and newborn $Nppc^{-/-}$/*SAP-Nppc-Tg* mice and their $Nppc^{-/-}$ littermates were dissected out and cultured for 4 d in Biggers, Gwatkin, Judah tissue culture medium for bone and cartilage (Invitrogen, Carlsbad, CA) with BSA (6 mg/ml; Wako Pure Chemical Industries, Ltd., Osaka, Japan), ascorbic acid (150 μg/ml; Wako), and penicillin/streptomycin (10,000 U/ml; Wako) in 12-well plates. Tibias from newborn $Nppc^{-/-}$ mice were incubated with vehicle or CNP at the dose of 10^{-9}, 10^{-8}, or 10^{-7} M for 4 d. At the end of the culture period, the longitudinal length of tibial explants was measured using a linear ocular scale mounted on a dissecting microscope at ×10 magnification.

Skeletal analysis

Mice were subjected to soft x-ray analysis (30 kVp, 5 mA for 1 min; Softron type SRO-M5; Softron, Tokyo, Japan), and the lengths of bones were measured on the soft x-ray film.

Histological analysis

For light microscopy, sections were cut from paraffin-embedded specimens. For Alcian Blue-hematoxylin and eosin (HE) staining, sections were deparaffinized with xylene and rehydrated through an ethanol series and distilled water. The sections were treated with 3% acetic acid for 3 min and Alcian Blue (Muto Pure Chemicals Co., Ltd., Tokyo, Japan) for 20 min. Then they were treated with hematoxylin (Muto) for 2 min, eosin alcohol (Muto) for 1 min, dehydrated, and then mounted with malinol (Muto).

As for *in situ* hybridization analyses for type II and type X collagens, 414- and 658-bp DNA fragments corresponding to the nucleotide positions 138-551 and 2893-3550 of mouse *Col2a1* and *Col10a1* cDNA (GenBank accession no. NM_031163 and 009925), respectively, were subcloned into pGEMT-Easy vector (Promega, Madison, WI) and were used for the generation of sense or antisense RNA probes. Digoxigenin (DIG)-labeled RNA probes were prepared with DIG RNA labeling mix (Roche, Stockholm, Sweden). Paraffin-embedded sections were hybridized with DIG-labeled RNA probes at 60 C for 16 h. The bound label was detected using 4-nitro blue tetrazolium chloride-5-bromo-4-chloro-3-indoyl-phosphate, 4-toluidine salt, an alkaline phosphate color substrate. The sections were counterstained with Kernechtrot (Muto).

For immunohistochemical detection of proliferating cell nuclear antigen (PCNA), tissue sections were incubated with mouse

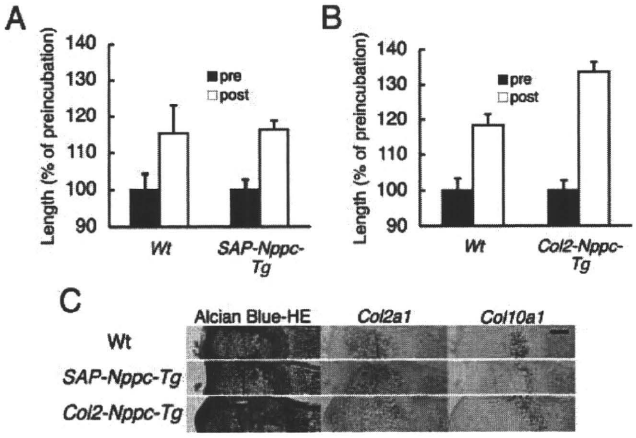

FIG. 1. Organ culture experiments using tibial explants from two different CNP transgenic mice. A and B, Graphs indicating percent of the longitudinal lengths of tibial explants at the end of incubation (*white bars*) compared by those of tibial explants at the beginning of incubation (*black bars*). Fetal (GD16) wild-type (Wt) *vs. SAP-Nppc-Tg* explants (A), and neonatal wild-type (Wt) *vs. Col2-Nppc-Tg* explants (B) are shown. C, Histological pictures of the growth plates of tibial explants at the end of 4-d culture period. From *top* to *bottom*, pictures of wild-type (Wt), *SAP-Nppc-Tg*, and *Col2-Nppc-Tg* explants are shown. *Left three panels* exhibit Alcian Blue-hematoxylin and eosin (HE) staining, and *middle three* and *right three panels* show *in situ* hybridization analyses for type II collagen (*Col2a1*) and type X collagen (*Col10a1*), respectively. *Scale bar*, 100 μm.

monoclonal anti-PCNA antibody (Dako, Glostrup, Denmark), and immunostaining was performed using Histofine mouse stain kit (Nichirei Corp., Tokyo, Japan) according to the manufacturer's instructions. Under the microscope (×400), three visual fields in the proliferative chondrocyte zone of the growth plate were randomly selected, and all cells and PCNA-positive cells in each field were counted. Then labeling index was calculated as the mean of these three values. Terminal deoxynucleotidyl transferase-mediated deoxyuridine triphosphate nick end labeling staining was performed using *in situ* apoptosis detection kit (Takara Bio Inc., Otsu, Japan) according to the manufacturer's instruction.

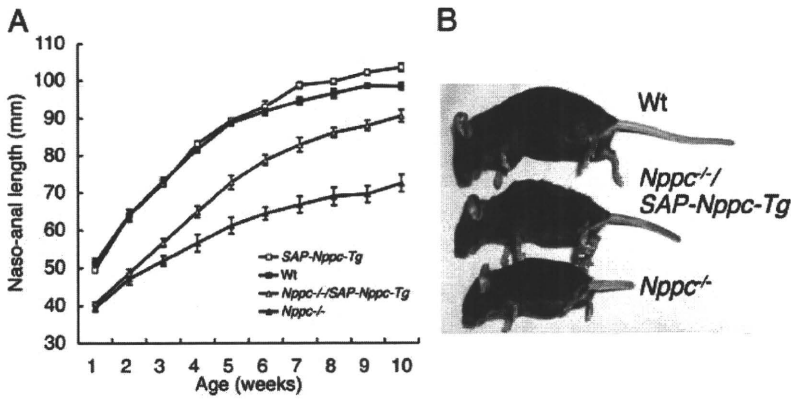

FIG. 2. Effect of circulating CNP on the longitudinal growth of $Nppc^{-/-}$ mice. A, Growth curves of nasoanal length of *SAP-Nppc-Tg* (*open square*), wild-type (*closed square*), $Nppc^{-/-}$/*SAP-Nppc-Tg* (*open triangle*), and $Nppc^{-/-}$ (*closed triangle*) mice. B, Gross appearance of wild-type (Wt), $Nppc^{-/-}$/*SAP-Nppc-Tg*, and $Nppc^{-/-}$ mice at the age of 15 wk.

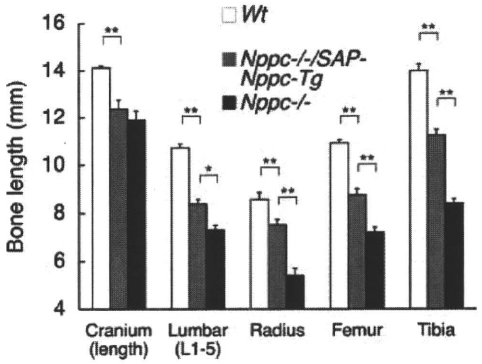

FIG. 3. Bone lengths of mice at the age of 3 wk measured on soft x-ray films. *White bars*, Wild-type mice; *gray bars*, $Nppc^{-/-}$/*SAP-Nppc-Tg* mice; *black bars*, $Nppc^{-/-}$ mice. *, $P < 0.05$; **, $P < 0.01$.

Statistical analysis

Data are expressed as means ± SE. The statistical significance of differences in mean values was assessed by Student's *t* test. The difference in survival rates among genotypes was assessed by Kaplan-Meier analysis.

Results

Organ culture experiments using tibial explants from *SAP-Nppc-Tg mice*

We generated two lines of CNP transgenic mice under the control of an SAP promoter, and both of them exhibited prominent skeletal overgrowth phenotype (14). We used one of them with milder skeletal phenotype as the *SAP-Nppc-Tg* mice for further experiments. To confirm whether the effect of *SAP-Nppc*-transgene on skeletal growth is humoral, we performed organ culture experiments by using tibias from *SAP-Nppc-Tg* mice and compared them with those from CNP transgenic mice with targeted overexpression of CNP in the cartilage by using mouse type II collagen promoter (*Col2-Nppc-Tg* mice) (5).

At the end of the 4-d culture period, the length of tibial explants from *SAP-Nppc-Tg* mice was not changed from that from their wild-type littermates, whereas the length of tibial explants from *Col2-Nppc-Tg* mice was about 13% larger than that from their wild-type littermates (Fig. 1, A and B). Histological analyses revealed that the widths of both nonhypertrophic and hypertrophic chondrocyte layers of the growth plates in *SAP-Nppc-Tg* explants, shown to express type II and type X collagens by *in situ* hybridization analyses, respectively, were not changed from those in wild-type explants, whereas they were larger in *Col2-Nppc-Tg* explants (Fig. 1C).

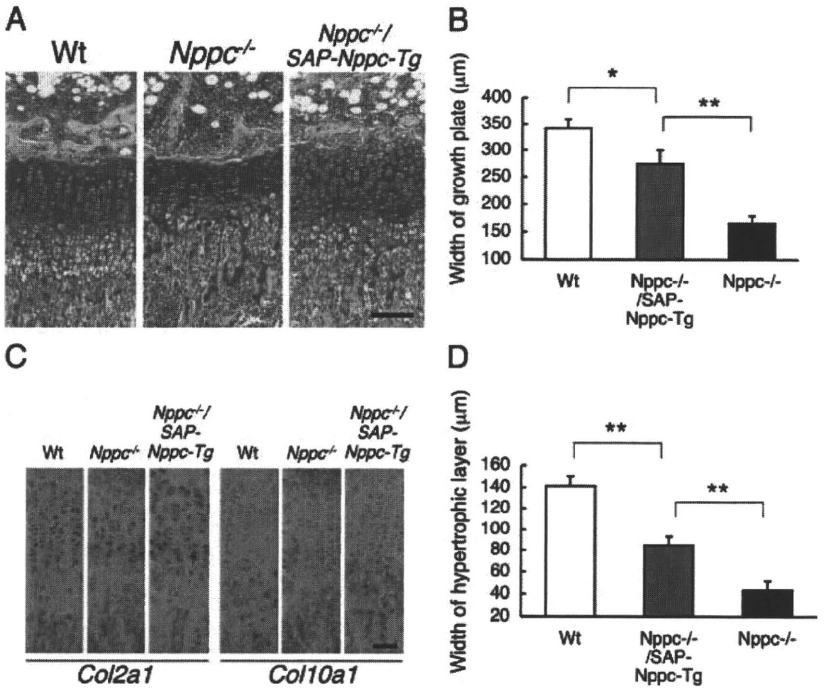

FIG. 4. Histological analyses of tibial growth plates of wild-type (Wt), *Nppc*$^{-/-}$, and *Nppc*$^{-/-}$*/SAP-Nppc-Tg* mice at the age of 3 wk. A, Histological pictures stained with Alcian Blue-hematoxylin and eosin (HE). *Scale bar*, 100 μm. B, Width of growth plates of tibias from wild-type (*white bar*), *Nppc*$^{-/-}$*/SAP-Nppc-Tg* (*gray bar*), and *Nppc*$^{-/-}$ (*black bar*) mice. *, $P < 0.05$; **, $P < 0.01$. C, Pictures of *in situ* hybridization analyses for type II collagen (*Col2a1*, *left three panels*) and type X collagen (*Col10a1*, *right three panels*). *Scale bar*, 50 μm. D, Width of hypertrophic chondrocyte layers of the growth plates of tibias from wild-type (*white bar*), *Nppc*$^{-/-}$*/SAP-Nppc-Tg* (*gray bar*), and *Nppc*$^{-/-}$ (*black bar*) mice. **, $P < 0.01$.

In addition, *in situ* hybridization analyses exhibited that the patterns and intensities of the staining for type II and type X collagens as the differentiation markers for nonhypertrophic and hypertrophic chondrocytes, respectively, were not different between in *SAP-Nppc-Tg* and wild-type explants. Furthermore, the proliferation of the growth plate chondrocytes in *SAP-Nppc-Tg* explants, estimated by immunohistochemical staining for PCNA, was almost the same as that in wild-type explants (labeling index: 60.4 ± 3.4 *vs.* 60.0 ± 2.4%). These results exhibit that CNP generated by *SAP-Nppc*-transgene affects endochondral bone growth in an endocrine manner.

The impaired endochondral bone growth of *Nppc*$^{-/-}$ mice was recovered by circulating CNP

Next we investigated the effect of circulating CNP on the chondrodysplastic phenotype of CNP knockout mice by crossing them with *SAP-Nppc-Tg* mice. Because *Nppc*$^{-/-}$ mice are thought to be infertile, we crossed *Nppc*$^{+/-}$ mice with *SAP-Nppc-Tg* mice and obtained *Nppc*$^{+/-}$*/SAP-Nppc-Tg* mice. Then these *Nppc*$^{+/-}$*/SAP-Nppc-Tg* mice were crossed with *Nppc*$^{+/-}$ mice to generate *Nppc*$^{-/-}$*/SAP-Nppc-Tg* mice.

At the first week after birth, *Nppc*$^{-/-}$*/SAP-Nppc-Tg* mice were smaller than their wild-type littermates, and the nasoanal length of *Nppc*$^{-/-}$*/SAP-Nppc-Tg* mice was almost the same as that of *Nppc*$^{-/-}$ mice (Fig. 2A). But they gradually became larger than *Nppc*$^{-/-}$ mice and became close to their wild-type littermates (Fig. 2, A and B). The nasoanal length of *Nppc*$^{-/-}$*/SAP-Nppc-Tg* mice was significantly larger than that of *Nppc*$^{-/-}$ mice at the age of 3 wk in male and at the age of 4 wk in female (male: 56.6 ± 1.1 mm and 51.9 ± 1.3 mm, respectively, n = 15 and 11 each, $P < 0.01$, and female: 63.3 ± 1.2 mm and 53.8 ± 0.7 mm, respectively, n = 10 and 10 each, $P < 0.01$). In accordance with the above observation, most bones formed through endochondral ossification in *Nppc*$^{-/-}$*/SAP-Nppc-Tg* mice grew longer than those in *Nppc*$^{-/-}$ mice. At the age of 3 wk, lumbar spine, radius, femur, and tibia of *Nppc*$^{-/-}$*/SAP-Nppc-Tg* mice were significantly longer than those of *Nppc*$^{-/-}$ mice, although they were still significantly shorter than those of their wild-type littermates (Fig. 3).

Histological analysis revealed that the width of the growth plate of tibias from *Nppc*$^{-/-}$*/SAP-Nppc-Tg* mice was significantly larger than that from *Nppc*$^{-/-}$ mice and was comparable with that from wild-type mice (Fig. 4, A and B). Width of every zone of the growth plate, especially that of hypertrophic chondrocyte zone expressing type X collagen as shown by *in situ* hybridization analysis, was significantly larger in *Nppc*$^{-/-}$*/SAP-Nppc-Tg* tibia than that in *Nppc*$^{-/-}$ tibia and was comparable with that in wild-type tibia (Fig. 4, A, C, and D).

The intensities or patterns of the staining for both type II and type X collagens by *in situ* hybridization were not different between that in *Nppc*$^{-/-}$*/SAP-Nppc-Tg* and that in *Nppc*$^{-/-}$ tibias, indicating that the differentiation for nonhypertrophic and hypertrophic chondrocytes in *Nppc*$^{-/-}$ growth plate was not affected by circulating CNP (Fig. 4C). Furthermore, immunohistochemical detection of PCNA revealed that the rate of PCNA-positive chondrocytes in *Nppc*$^{-/-}$*/SAP-Nppc-Tg* growth plate was not changed from that in *Nppc*$^{-/-}$ growth plate (labeling index: 23.0 ± 7.3 *vs.* 25.4 ± 1.4%), exhibiting that the proliferation of the chondrocytes in *Nppc*$^{-/-}$ growth plate was not altered by circulating CNP. In addition, we

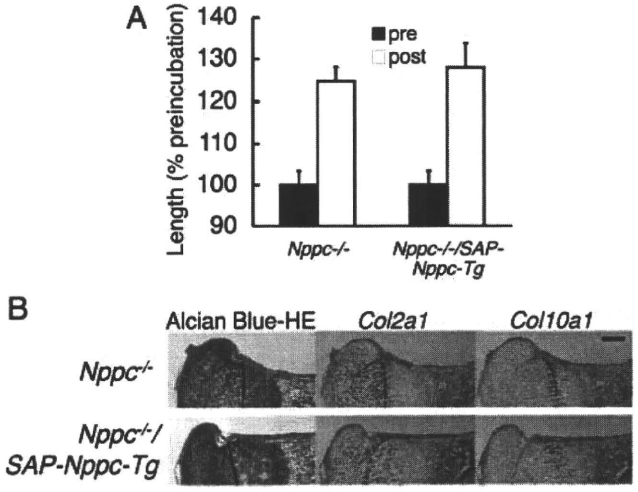

FIG. 5. Organ culture experiments using tibial explants from neonatal *Nppc*$^{-/-}$ and *Nppc*$^{-/-}$*/SAP-Nppc-Tg* mice. A, The graph indicating percent of the longitudinal length of tibial explants at the end of incubation (*white bars*) compared with that of tibial explants at the beginning of incubation (*black bars*). B, Histological analyses of the tibial explants at the end of the 4-d culture period. *Upper panels* show histological pictures of the growth plates of *Nppc*$^{-/-}$ explants, and *lower panels* show those of *Nppc*$^{-/-}$*/SAP-Nppc-Tg* explants. *Left panels* exhibit Alcian Blue-hematoxylin and eosin (HE) staining, and *middle* and *right panels* show *in situ* hybridization analyses for type II collagen (*Col2a1*) and type X collagen (*Col10a1*), respectively. *Scale bar*, 100 μm.

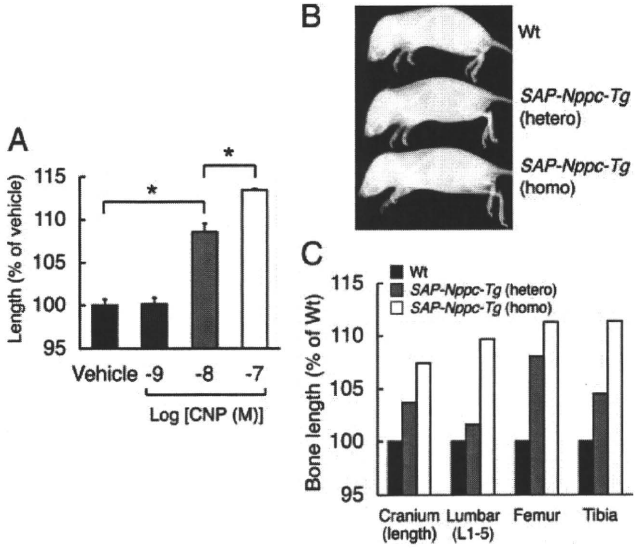

FIG. 6. Dose-dependent effect of circulating CNP on endochondral bone growth. A, Dose-dependent effect of addition of CNP on the growth of tibial explants from *Nppc*$^{-/-}$ mice in organ culture. The graph indicates percent of the longitudinal length of tibial explants incubated with indicated doses of CNP compared with that with vehicle, at the end of the 4-d culture period. *, $P < 0.05$. B, Soft x-ray picture of 3-wk-old wild-type (Wt) and *SAP-Nppc-Tg* mice with heterozygous (hetero) and homozygous (homo) *SAP-Nppc-Tg* transgene. Note that the nasoanal length is increased in accordance with the copy number of the transgene. C, The graph indicating percent of the length of each bone of heterozygous (*gray bar*) or homozygous (*white bar*) *SAP-Nppc-Tg* mice compared with that of wild-type mice (*black bar*) [n = 2 (Wt), four (hetero), and four (homo), each].

could scarcely find out the difference in the state of apoptosis of the growth plate chondrocytes between that in *Nppc*$^{-/-}$*/SAP-Nppc-Tg* and that in *Nppc*$^{-/-}$ tibias by terminal deoxynucleotidyl transferase-mediated deoxyuridine triphosphate nick end labeling staining (data not shown).

To further confirm whether the *SAP-Nppc*-transgene product humorally affects the endochondral bone growth in *Nppc*$^{-/-}$ mice, organ culture experiments using tibial explants from neonatal *Nppc*$^{-/-}$*/SAP-Nppc-Tg* and *Nppc*$^{-/-}$ mice were performed. At the end of the 4-d culture period, longitudinal length of tibial explants from *Nppc*$^{-/-}$*/SAP-Nppc-Tg* mice was not changed from that from *Nppc*$^{-/-}$ mice (Fig. 5A). Histological analyses revealed that the widths of both nonhypertrophic and hypertrophic chondrocyte layers of the growth plate, expressing type II and type X collagens, respectively, were not different between in *Nppc*$^{-/-}$*/SAP-Nppc-Tg* and *Nppc*$^{-/-}$ explants (Fig. 5B). Neither the differentiation (estimated by *in situ* hybridization analyses for type II and type X collagens, Fig. 5B) nor the proliferation (evaluated by PCNA analysis, labeling index: 41.0 ± 3.3 *vs.* 44.9 ± 3.0%) of the growth plate chondrocytes was different between that in *Nppc*$^{-/-}$*/SAP-Nppc-Tg* and that in *Nppc*$^{-/-}$ explants.

To investigate whether the stimulatory effect of circulating CNP on the endochondral bone growth of *Nppc*$^{-/-}$ mice is dose dependent, we studied the effect of CNP on the growth of tibial explants from neonatal *Nppc*$^{-/-}$ mice in organ culture experiment. As shown in Fig. 6A, the growth of tibial explants from *Nppc*$^{-/-}$ mice was stimulated by addition of CNP in a dose-dependent manner. Furthermore, we generated *SAP-Nppc-Tg* mice with homozygous *SAP-Nppc* transgene to confirm a dose-dependent effect of circulating CNP on endochondral bone growth *in vivo*.

At the age of 3 wk, soft x-ray analyses revealed that the longitudinal body length and the growth of every bone formed through endochondral bone growth were promoted in accordance with the copy number of *SAP-Nppc* transgene, indicating the dose-dependent effect of circulating CNP on endochondral bone growth *in vivo* (Fig. 6B). Collectively, these results suggest that circulating CNP would cure the impaired skeletal growth of *Nppc*$^{-/-}$ mice in a dose-dependent manner *in vivo*.

Effects of increased circulating CNP on the body weight gain and the survival rate of *Nppc*$^{-/-}$ mice

We also investigated the effects of circulating CNP on other aspects of the impaired growth of chondrodysplastic *Nppc*$^{-/-}$ mice. The body weight of *Nppc*$^{-/-}$*/SAP-Nppc-Tg* mice was smaller than that of their wild-type littermates and was comparable with that of their *Nppc*$^{-/-}$ littermates at the age of 1 wk (Fig. 7A). However, *Nppc*$^{-/-}$*/SAP-Nppc-Tg* mice gradually became heavier

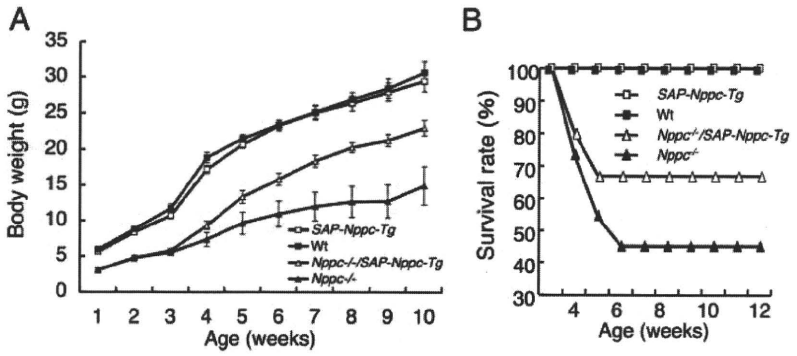

FIG. 7. Effect of circulating CNP on the body weight and the survival rate of $Nppc^{-/-}$ mice. A, Growth curves of body weight of *SAP-Nppc-Tg* (*open square*), wild-type (Wt; *closed square*), $Nppc^{-/-}$/*SAP-Nppc-Tg* (*open triangle*), and $Nppc^{-/-}$ (*closed triangle*) mice. B, Survival curves of *SAP-Nppc-Tg* (*open square*), wild-type (*closed square*), $Nppc^{-/-}$/*SAP-Nppc-Tg* (*open triangle*), and $Nppc^{-/-}$ (*closed triangle*) mice.

than their $Nppc^{-/-}$ littermates (Fig. 7A), and the body weight of $Nppc^{-/-}$/*SAP-Nppc-Tg* mice was significantly larger than their wild-type littermates at the age of 4 wk in males and 3 wk in females (males: 9.3 ± 0.5 g and 7.3 ± 0.9 g, respectively, n = 12 and 7 each, $P < 0.05$, and females: 5.4 ± 0.1 g and 4.7 ± 0.2 g, respectively, n = 11 and 12 each, $P < 0.05$). On the other hand, there was no difference in body weight between the *SAP-Nppc-Tg* and wild-type mice, albeit *SAP-Nppc-Tg* mice became larger than the wild-type mice in nasoanal length (Figs. 2A and 6).

We have previously reported that the survival rate of $Nppc^{-/-}$ mice greatly drops before adulthood, albeit the genotype ratio of $Nppc^{-/-}$ mice on d 16.5 of pregnancy is in accord with Mendelian proportion (1). In this study, analysis of intercrosses between $Nppc^{+/-}$/*SAP-Nppc-Tg* mice and $Nppc^{+/-}$ mice revealed that the genotype ratios of wild type to $Nppc^{+/-}$ to $Nppc^{-/-}$ and *SAP-Nppc-Tg* to $Nppc^{+/-}$/*SAP-Nppc-Tg* to $Nppc^{-/-}$/*SAP-Nppc-Tg* at weaning (3 wk of age) are 1:2.78:1 and 1:2.71:1.24 (total n = 104 and 110), respectively, indicating expected Mendelian proportions. As have we previously reported, the survival rate of $Nppc^{-/-}$ mice dropped to about 40% before adulthood (Fig. 7B). However, the survival rate of $Nppc^{-/-}$/*SAP-Nppc-Tg* mice was greatly improved compared with that of $Nppc^{-/-}$ mice (Fig. 7B).

Discussion

In the present study, we investigated the endocrine effects of CNP on chondrodysplastic CNP knockout mice by using *SAP-Nppc-Tg* mice.

In the organ culture experiments, the growth of *SAP-Nppc-Tg* tibias was not changed from that of wild-type tibias, whereas the growth of *Col2-Nppc-Tg* tibias was strongly promoted compared with that of wild-type tibias. This result confirms that the growth stimulating effect of bones formed through endochondral ossification in *SAP-Nppc-Tg* mice is not autocrine/paracrine but endocrine effect of CNP, which is produced by the *SAP-Nppc* transgene. Because we expected that we would observe the effect of circulating CNP on endochondral bone growth clearly in a state without basal CNP effect, we then investigated whether or not elevation of circulating CNP could recover the impaired endochondral bone growth caused by depletion of CNP in mice *in vivo*. Decreased width of the growth plate observed in $Nppc^{-/-}$ mice was recovered in $Nppc^{-/-}$/*SAP-Nppc-Tg* mice, and accordingly, impaired endochondral bone growth observed in $Nppc^{-/-}$ mice was considerably and significantly recovered in $Nppc^{-/-}$/*SAP-Nppc-Tg* mice.

The endocrine effect of CNP produced by the *SAP-Nppc* transgene in $Nppc^{-/-}$/*SAP-Nppc-Tg* mice was further confirmed by the organ culture experiments in that the growth of $Nppc^{-/-}$/*SAP-Nppc-Tg* tibias was not changed from that of $Nppc^{-/-}$ tibias. These results clearly indicate that CNP can humorally affect endochondral bone growth. Furthermore, the result of the organ culture experiment using $Nppc^{-/-}$ bones (Fig. 6A) and the gene-dose effect of *SAP-Nppc* transgene on bone growth *in vivo* (Fig. 6B, C) suggest that the endocrine effect of CNP on endochondral bone growth is dose dependent.

Chondrodysplasia is composed of many different forms of genetic disorders characterized by impaired endochondral bone growth (7, 17). Because the CNP/GC-B system plays a crucial role in endochondral bone growth, loss of function mutations in the genes coding for molecules related to the CNP/GC-B system could cause chondrodysplasia. In fact, recent studies have revealed that mutations in the gene encoding human GC-B cause one form of chondrodysplasia, acromesomelic dysplasia type Maroteaux (18, 19).

In mice, loss of function mutations in the GC-B gene cause impaired skeletal growth in spontaneous mutant *cn/cn* and short-limbed dwarfism (*slw/slw*) mice (20, 21). As for spontaneous mutations in other genes related to the CNP/GC-B system, a mutation in the gene coding for cGMP-dependent protein kinase type II, an important downstream mediator of the CNP/GC-B system, causes impaired endochondral bone growth in Komeda miniature rat Ishikawa (22, 23). Furthermore, recent studies have elucidated that a spontaneous loss of function mutation in the murine CNP gene causes impaired skeletal growth observed in the long bone abnormality (*lbab/lbab*) mice (24–26).

Just as in the case with rodents, any forms of human chondrodysplasia might be caused by mutations in the cGMP-dependent protein kinase type II or CNP gene, albeit they are not yet discovered. In case a form of human chondrodysplasia caused by a mutation in the CNP gene is discovered in future, CNP knockout mice would be a novel mice model of human chondrodysplasia. On the other hand, spontaneous GC-B mutant (*cn/cn* and *slw/slw*) mice and GC-B knockout mice are regarded as mice models of acromesomelic dysplasia type Maroteaux, and impaired skeletal growth of these mice would not be recovered by crossing them with *SAP-Nppc-Tg* mice. This notion is supported by the result of the organ culture experiment, in which tibial explants from fetal GC-B knockout mice are not increased in length by addition of CNP (4).

We previously reported that the impaired skeletal growth of achondroplastic model mice was almost completely recovered by crossing them with *SAP-Nppc-Tg* mice (16). The impairment of skeletal growth of the achondroplastic model mice that we used in our previous study was considerably mild compared with that of $Nppc^{-/-}$ mice: the nasoanal length of the achondroplastic model mice was about 10% shorter than that of wild-type mice at the age of 10 wk (14), whereas the nasoanal length of $Nppc^{-/-}$ mice was about 30% shorter than that of wild-type mice. The reason that the impaired skeletal growth of $Nppc^{-/-}$ mice was not completely rescued in $Nppc^{-/-}$/*SAP-Nppc-Tg* mice in our present study might be because the low graded elevation of the plasma CNP concentrations in *SAP-Nppc-Tg* mice (about 1.8 times higher than those in wild-type mice) was not sufficient for the complete rescue of severe skeletal phenotype of $Nppc^{-/-}$ mice, whereas it was enough to cure the mild skeletal impairment of the achondroplastic model mice. Although about 2 times of elevation of plasma CNP concentrations can stimulate bone growth in *SAP-Nppc-Tg* mice (14) or human with a chromosomal translocation (27), higher plasma concentration of CNP might be needed for the complete treatment of impaired bone growth in chondrodysplasia.

As for the mechanism of the skeletal rescue of CNP knockout mice by circulating CNP, the differentiation and the proliferation of the growth plate chondrocytes of $Nppc^{-/-}$/*SAP-Nppc-Tg* mice were not changed from those of $Nppc^{-/-}$ mice. This result coincides with our previous observation that CNP does not so strongly affect differentiation and proliferation of the growth plate chondrocytes *in vivo* (5, 14). On the other hand, proteoglycan synthesis is greatly increased in the growth plate of *SAP-Nppc-Tg* mice (14), so we speculate that the shortened $Nppc^{-/-}$ growth plate is restored by circulating CNP in $Nppc^{-/-}$/*SAP-Nppc-Tg* mice through the recovery of matrix synthesis, resulting in the recovery of endochondral bone growth.

The impaired growth of $Nppc^{-/-}$ mice was recovered in not only longitudinal length but also body weight, and furthermore, the mortality of $Nppc^{-/-}$ mice was greatly decreased, by circulating CNP. Together with our previous results that targeted overexpression of CNP in the cartilage of $Nppc^{-/-}$ mice improved not only their impaired longitudinal growth but also their impaired body weight gain and that prolonged their survival (1), we consider that the recovery from the impaired endochondral bone growth in $Nppc^{-/-}$ mice by circulating CNP resulted in the recovery of overall growth and also in longevity. The mechanisms through which recovery in skeletal growth results in the recovery of overall growth and the prolonged survival are not yet elucidated. One of the possibilities is that the malformation in the maxillofacial region of $Nppc^{-/-}$ mice, which is caused by impaired endochondral ossification, may disturb their teeth coming together correctly: this condition may prevent them from eating enough and lead them to malnutrition. Further investigation of the craniofacial phenotype of $Nppc^{-/-}$ mice is now ongoing in our laboratory (Nakao, K., Y. Okubo, N. Koyama, K. Osawa, M. Miura, A. Yasoda, K. Nakao, and K. Bessho, manuscript in preparation).

In conclusion, we have revealed that circulating CNP rescues the impaired growth and early death of chondrodysplastic CNP knockout mice through the recovery of endochondral bone growth. We have started to apply the strong stimulatory effect of the CNP/GC-B system on endochondral bone growth to the treatment of chondrodysplasias (16) for those no effective drug therapy is available to date. The results of our present paper suggest that systemic administration of CNP or its analog, which would stimulate GC-B, might have therapeutic potential against not only impaired skeletal growth but also other aspects of impaired growth including impaired body weight gain in patients suffering from chondrodysplasias and might resultantly protect them from their early death.

Acknowledgments

We thank Chugai Pharmaceutical Co. for *SAP-Nppc-Tg* mice and Asubio Pharma Co. for *Col2-Nppc-Tg* mice.

Address all correspondence and requests for reprints to: Akihiro Yasoda, M.D., Ph.D., 54 Shogoin-Kawahara-cho, Sakyo-ku, Kyoto, 606-8507, Japan. E-mail: yasoda@kuhp.kyoto-u.ac.jp.

This work was supported by a Grant-in-Aid for Scientific Research from the Ministry of Health, Labor, and Welfare of Japan and the Ministry of Education, Culture, Sports, Sciences, and Technology of Japan (Grant 19591075).

Disclosure Summary: T.F., Y.K., E.K., T.Y., T.N., N.K., M.Mi., N.T., H.A., and M.Mu. have nothing to declare. A.Y. receives grant support (2008.12.1-2011.11.30) from Chugai Pharmaceutical Co., Ltd. K.N. is an inventor of related U.S. patent (US6743425) and patent applications in Japan (woo3-113116, 2003-104908), Canada (CA2398030), and Brazil (BR200203172).

References

1. **Chusho H, Tamura N, Ogawa Y, Yasoda A, Suda M, Miyazawa T, Nakamura K, Nakao K, Kurihara T, Komatsu Y, Itoh H, Tanaka K, Saito Y, Katsuki M, Nakao K** 2001 Dwarfism and early death in mice lacking C-type natriuretic peptide. Proc Natl Acad Sci USA 98:4016–4021
2. **Yasoda A, Ogawa Y, Suda M, Tamura N, Mori K, Sakuma Y, Chusho H, Shiota K, Tanaka K, Nakao K** 1998 Natriuretic peptide regulation of endochondral ossification. Evidence for possible roles of the C-type natriuretic peptide/guanylyl cyclase-B pathway. J Biol Chem 273:11695–11700
3. **Suga S, Nakao K, Hosoda K, Mukoyama M, Ogawa Y, Shirakami G, Arai H, Saito Y, Kambayashi Y, Inouye K, Imura H** 1992 Receptor selectivity of natriuretic peptide family, atrial natriuretic peptide, brain natriuretic peptide, and C-type natriuretic peptide. Endocrinology 130:229–239
4. **Tamura N, Doolittle LK, Hammer RE, Shelton JM, Richardson JA, Garbers DL** 2004 Critical roles of the guanylyl cyclase B receptor in endochondral ossification and development of female reproductive organs. Proc Natl Acad Sci USA 101:17300–17305
5. **Yasoda A, Komatsu Y, Chusho H, Miyazawa T, Ozasa A, Miura M, Kurihara T, Rogi T, Tanaka S, Suda M, Tamura N, Ogawa Y, Nakao K** 2004 Overexpression of CNP in chondrocytes rescues achondroplasia through a MAPK-dependent pathway. Nat Med 10: 80–86
6. **Miyazawa T, Ogawa Y, Chusho H, Yasoda A, Tamura N, Komatsu Y, Pfeifer A, Hofmann F, Nakao K** 2002 Cyclic GMP-dependent protein kinase II plays a critical role in C-type natriuretic peptide-mediated endochondral ossification. Endocrinology 143:3604–3610
7. **Superti-Furga A, Bonafé L, Rimoin DL** 2001 Molecular-pathogenetic classification of genetic disorders of the skeleton. Am J Med Genet 106:282–293
8. **Naski MC, Colvin JS, Coffin JD, Ornitz DM** 1998 Repression of hedgehog signaling and BMP4 expression in growth plate cartilage by fibroblast growth factor receptor 3. Development 125:4977–4988
9. **Rousseau F, Bonaventure J, Legeai-Mallet L, Pelet A, Rozet JM, Maroteaux P, Le Merrer M, Munnich A** 1994 Mutations in the gene encoding fibroblast growth factor receptor-3 in achondroplasia. Nature 371:252–254
10. **Mukoyama M, Nakao K, Hosoda K, Suga S, Saito Y, Ogawa Y, Shirakami G, Jougasaki M, Obata K, Yasue H, Kambayashi Y, Inouye K, Imura H** 1991 Brain natriuretic peptide as a novel cardiac hormone in humans. Evidence for an exquisite dual natriuretic peptide system, atrial natriuretic peptide and brain natriuretic peptide. J Clin Invest 87:1402–1412
11. **Ogawa Y, Nakao K, Mukoyama M, Hosoda K, Shirakami G, Arai H, Saito Y, Suga S, Jougasaki M, Imura H** 1991 Natriuretic peptides as cardiac hormones in normotensive and spontaneously hypertensive rats. The ventricle is a major site of synthesis and secretion of brain natriuretic peptide. Circ Res 69:491–500
12. **Komatsu Y, Nakao K, Suga S, Ogawa Y, Mukoyama M, Arai H, Shirakami G, Hosoda K, Nakagawa O, Hama N, Imura H** 1991 C-type natriuretic peptide (CNP) in rats and humans. Endocrinology 129:1104–1106
13. **Suga S, Nakao K, Itoh H, Komatsu Y, Ogawa Y, Hama N, Imura H** 1992 Endothelial production of C-type natriuretic peptide and its marked augmentation by transforming growth factor-β. Possible existence of "vascular natriuretic peptide system." J Clin Invest 90: 1145–1149
14. **Kake T, Kitamura H, Adachi Y, Yoshioka T, Watanabe T, Matsushita H, Fujii T, Kondo E, Tachibe T, Kawase Y, Jishage K, Yasoda A, Mukoyama M, Nakao K** 2009 Chronically elevated plasma C-type natriuretic peptide level stimulates skeletal growth in transgenic mice. Am J Physiol Endocrinol Metab 297:E1339–E1348
15. **Ogawa Y, Itoh H, Tamura N, Suga S, Yoshimasa T, Uehira M, Matsuda S, Shiono S, Nishimoto H, Nakao K** 1994 Molecular cloning of the complementary DNA and gene that encode mouse brain natriuretic peptide and generation of transgenic mice that overexpress the brain natriuretic peptide gene. J Clin Invest 93:1911–1921
16. **Yasoda A, Kitamura H, Fujii T, Kondo E, Murao N, Miura M, Kanamoto N, Komatsu Y, Arai H, Nakao K** 2009 Systemic administration of C-type natriuretic peptide as a novel therapeutic strategy for skeletal dysplasias. Endocrinology 150:3138–3144
17. **Superti-Furga A, Unger S** 2007 Nosology and classification of genetic skeletal disorders: 2006 revision. Am J Med Genet A 143:1–18
18. **Bartels CF, Bükülmez H, Padayatti P, Rhee DK, van Ravenswaaij-Arts C, Pauli RM, Mundlos S, Chitayat D, Shih LY, Al-Gazali LI, Kant S, Cole T, Morton J, Cormier-Daire V, Faivre L, Lees M, Kirk J, Mortier GR, Leroy J, Zabel B, Kim CA, Crow Y, Braverman NE, van den Akker F, Warman ML** 2004 Mutations in the transmembrane natriuretic peptide receptor NPR-B impair skeletal growth and cause acromesomelic dysplasia, type Maroteaux. Am J Hum Genet 75:27–34
19. **Hachiya R, Ohashi Y, Kamei Y, Suganami T, Mochizuki H, Mitsui N, Saitoh M, Sakuragi M, Nishimura G, Ohashi H, Hasegawa T, Ogawa Y** 2007 Intact kinase homology domain of natriuretic peptide receptor-B is essential for skeletal development. J Clin Endocrinol Metab 92:4009–4014
20. **Tsuji T, Kunieda T** 2005 A loss-of-function mutation in natriuretic peptide receptor 2 (*Npr2*) gene is responsible for disproportionate dwarfism in cn/cn mouse. J Biol Chem 280:14288–14292
21. **Sogawa C, Tsuji T, Shinkai Y, Katayama K, Kunieda T** 2007 Short-limbed dwarfism: slw is a new allele of Npr2 causing chondrodysplasia. J Hered 98:575–580
22. **Chikuda H, Kugimiya F, Hoshi K, Ikeda T, Ogasawara T, Shimoaka T, Kawano H, Kamekura S, Tsuchida A, Yokoi N, Nakamura K, Komeda K, Chung UI, Kawaguchi H** 2004 Cyclic GMP-dependent protein kinase II is a molecular switch from proliferation to hypertrophic differentiation of chondrocytes. Genes Dev 18:2418–2429
23. **Kawasaki Y, Kugimiya F, Chikuda H, Kamekura S, Ikeda T, Kawamura N, Saito T, Shinoda Y, Higashikawa A, Yano F, Ogasawara T, Ogata N, Hoshi K, Hofmann F, Woodgett JR, Nakamura K, Chung UI, Kawaguchi H** 2008 Phosphorylation of GSK-3β by cGMP-dependent protein kinase II promotes hypertrophic differentiation of murine chondrocytes. J Clin Invest 118:2506–2515
24. **Jiao Y, Yan J, Jiao F, Yang H, Donahue LR, Li X, Roe BA, Stuart J, Gu W** 2007 A single nucleotide mutation in Nppc is associated with a long bone abnormality in lbab mice. BMC Genet 8:16
25. **Tsuji T, Kondo E, Yasoda A, Inamoto M, Kiyosu C, Nakao K, Kunieda T** 2008 Hypomorphic mutation in mouse *Nppc* gene causes retarded bone growth due to impaired endochondral ossification. Biochem Biophys Res Commun 376:186–190
26. **Yoder AR, Kruse AC, Earhart CA, Ohlendorf DH, Potter LR** 2008 Reduced ability of C-type natriuretic peptide (CNP) to activate natriuretic peptide receptor B (NPR-B) causes dwarfism in lbab$^{-/-}$ mice. Peptides 29:1575–1581
27. **Bocciardi R, Giorda R, Buttgereit J, Gimelli S, Divizia MT, Beri S, Garofalo S, Tavella S, Lerone M, Zuffardi O, Bader M, Ravazzolo R, Gimelli G** 2007 Overexpression of the C-type natriuretic peptide (CNP) is associated with overgrowth and bone anomalies in an individual with balanced t(2;7) translocation. Hum Mutat 28:724–731

Establishment of a Novel Ghrelin-Producing Cell Line

Hiroshi Iwakura, Yushu Li, Hiroyuki Ariyasu, Hiroshi Hosoda, Naotetsu Kanamoto, Mika Bando, Go Yamada, Kiminori Hosoda, Kazuwa Nakao, Kenji Kangawa, and Takashi Akamizu

Ghrelin Research Project (H.I., Y.L., H.A., M.B., T.A.), Translational Research Center, and Department of Medicine and Clinical Science, Endocrinology, and Metabolism (N.K., G.Y., K.H., K.N.), Kyoto University Hospital, Kyoto University Graduate School of Medicine, Kyoto 606-8507, Japan; and National Cardiovascular Center Research Institute (H.H., K.K.), Osaka 565-8565, Japan

To establish a tool to study ghrelin production and secretion *in vitro*, we developed a novel ghrelin-producing cell line, MGN3–1 (mouse ghrelinoma 3-1) cells from a gastric ghrelin-producing cell tumor derived from ghrelin-promoter Simian virus 40-T-antigen transgenic mice. MGN3-1 cells preserve three essential characteristics required for the *in vitro* tool for ghrelin research. First, MGN3-1 cells produce a substantial amount of ghrelin at levels approximately 5000 times higher than that observed in TT cells. Second, MGN3-1 cell expressed two key enzymes for acyl modification and maturation of ghrelin, namely ghrelin *O*-acyltransferase for acylation and prohormone convertase 1/3 for maturation and the physiological acyl modification and maturation of ghrelin were confirmed. Third, MGN3-1 cells retain physiological regulation of ghrelin secretion, at least in regard to the suppression by somatostatin and insulin, which is well established in *in vivo* studies. Thus, MGN3-1 cells are the first cell line derived from a gastric ghrelin-producing cell preserving secretion of substantial amounts of ghrelin under physiological regulation. This cell line will be a useful tool for both studying the production and secretion of ghrelin and screening of ghrelin-modulating drugs. (***Endocrinology* 151: 2940–2945, 2010**)

Ghrelin, a stomach-derived hormone, is composed of 28 amino acid residues with unique acyl-modification (1). Plasma ghrelin levels are regulated by acute and chronic energy status: serum levels are increased during a postprandial period and decreased after refeeding (2, 3). Ghrelin levels are low in obese individuals and high in lean people (4, 5). The direct factors regulating ghrelin secretion from ghrelin-producing cells (X/A-like cells), however, are not fully understood.

One method to investigate the direct effect of a specific factor on ghrelin secretion is to use a ghrelin-producing cell line. Ghrelin production has been reported by several cell lines, including TT (6), HL-60, THP-1, SupT1 (7), and HELL (8) cells. All of these cell lines differ completely from endogenous ghrelin-producing cells. TT cells originate from human thyroid medullary cancer, whereas HL-60, SupT1, and HELL cells are leukocyte in origin, with HELL being erythroleukemic line. Although these cell lines may be used to study ghrelin production (9), they are not ideal tools to study the regulation of ghrelin secretion. Therefore, establishment of a cell line originating from ghrelin-producing cells of the stomach would be useful for studying ghrelin production and secretion. Furthermore, it is vital to establish such cell line for studying factors directly affecting ghrelin production and secretion.

In this study, we established a ghrelin-producing cell line from a gastric tumor derived from ghrelin-promoter-Simian virus 40 T-antigen transgenic (GP-Tag Tg) mice.

Materials and Methods

Animals

GP-Tag Tg mice were generated as described previously (10). KSN nude mice were purchased from Shimizu Laboratory Supplies (Kyoto, Japan). Animals were maintained on

ISSN Print 0013-7227 ISSN Online 1945-7170
Printed in U.S.A.

doi: 10.1210/en.2010-0090 Received January 22, 2010. Accepted March 12, 2010.
First Published Online April 7, 2010

Abbreviations: AA, Amino acid; FBS, fetal bovine serum; GOAT, ghrelin *O*-acyltransferase; GP-Tag Tg, ghrelin-promoter-Simian virus 40 T-antigen transgenic; KRB, Krebs-Ringer buffer; PC, prohormone convertase; siRNA, small interfering RNA.

standard rodent food (CE-2, 352 kcal/100 g; Japan CLEA, Tokyo, Japan) on a 12-h light, 12-h dark cycle unless otherwise indicated. All experimental procedures were approved by the Kyoto University Graduate School of Medicine Committee on Animal Research.

Cell culture

A gastric tumor resected from a GP-Tag Tg mouse was minced and digested with the combination of 1.5 mg/ml collagenase type I (Sigma-Aldrich, St. Louis, MO) and 0.5 mg/ml dispase (Roche, Basel, Switzerland) in DMEM (11995-065; Life Technologies, Inc., Carlsbad, CA) supplemented with 10% fetal bovine serum (FBS) at 37 C for 90 min. After washing with PBS, tumor cells were cultured in DMEM supplemented with 10% FBS, 100 U/ml penicillin, and 100 μg/ml streptomycin at 37 C in 10% CO_2. Stromal cells were diminished by serial passage of tumor cells into new dishes 2–3 h after seeding the cells to the first dishes. After several passages of cells in 3-d intervals, the cells were cloned by dilution cloning onto a feeder layer of mitomycin-C-treated embryonic fibroblasts in 96-well microplates.

TT cells were cultured in Ham's F-12K supplemented with 10% FBS at 37 C in 5% CO_2 as described previously (6).

Immunocytochemistry

Cells were cultured in a chamber slide system (Nulge Nunc, Rochester, NY) and then fixed with 10% formalin for 15 min. Formalin-fixed slides were immunostained using the avidin-biotin peroxidase complex method (Vectastain ABC Elite kit; Vector Laboratories, Burlingame, CA) as described previously (11). Slides were incubated with anti-carboxy (C)-terminal ghrelin (amino acid, AA: 13-28) (12) (1:2000 at final dilution), which detects both ghrelin and desacyl-ghrelin, amino N-terminal ghrelin (12) that recognizes the *n*-octanoylated portion of ghrelin (AA: 1–11; 1:5000), antiglucagon (1:500) (Dako, Glostrup, Denmark), antisomatostatin (1:500) (Dako), and antigastrin (1:500) (Dako).

Electron microscope

Electron microscope study was performed as described previously (13). Cell pellets were fixed with 1% glutaraldehyde at 4 C for 2 h. After washing in phosphate buffer, samples were postfixed with 2% OsO_4 at 4 C for 2 h dehydrated with ethanol and embedded in Quetol 812 (Nisshin EM, Tokyo, Japan). Ultrathin sections of samples were cut, stained with uranyl acetate for 15 min followed by lead acetate for 5 min, and then viewed with an H-300 electron microscope (Hitachi, Tokyo, Japan).

Measurements of ghrelin concentrations in cells and culture medium

Cells were detached from dishes in enzyme-free cell dissociation buffer (Life Technologies). After centrifugation, cells were dissolved in PBS and boiled for 5 min. Acetic acid was added to each solution to a final concentration of 1 M. After needle shearing and centrifugation, the cell supernatants were applied to Sep-Pak C18 cartridges (Waters Corp., Milford, MA) preequilibrated with 0.9% saline. Cartridges were washed in saline and 5% CH_3CN/0.1% trifluoroacetic acid and eluted with 60% CH_3CN/0.1% trifluoroacetic acid. Eluates were lyophilized and subjected to ghrelin RIA. To measure ghrelin concentrations in culture medium, the collected culture media were centrifuged, and the resulting supernatants were immediately applied to Sep-Pak C18 cartridges and processed as described above. RIAs were performed using anti-C-terminal ghrelin (AA: 13–28) antiserum (C-RIA), which detects both ghrelin and desacyl-ghrelin, and anti-N-terminal ghrelin (AA: 1–11) antiserum (N-RIA), which detects ghrelin only, as described previously (12, 14).

RT-PCR and quantitative RT-PCR

Total RNA was extracted using a Sepasol-RNA kit (Nacalai Tesque, Kyoto, Japan). Reverse transcription was performed with a high-capacity cDNA reverse transcriptase kit (Applied Biosystems, Foster City, CA). RT-PCR was performed using a GeneAmp 9700 cycler (Applied Biosystems) with Amplitaqgold using appropriate primers (Supplemental Table 1 published on The Endocrine Society's Journals Online web site at http://endo.endojournals.org). Real-time quantitative PCR was performed using an ABI PRISM 7500 sequence detection system (Applied Biosystems) using appropriate primers and TaqMan probes or with Power SybrGreen (Supplemental Table 1). The mRNA expression of each gene was normalized to levels of 18S rRNA.

Western blotting

The molecular size of ghrelin in the medium was determined by tricine SDS-PAGE and Western blot analysis as described previously (10). MGN3-1 cells were seeded in 10-cm dishes (5.0×10^6 cells/dish). Culture media were collected after a 3-d incubation and subjected to HPLC purification and lyophilization as described above. Tricine SDS-PAGE and Western blot analysis were performed as described previously using anti-COOH-terminal ghrelin antibody (1:5000) (10).

Reverse-phase HPLC

MGN3-1 cells were seeded in a six-well dish (5×10^5 cells/well). After a washing in PBS, cells were incubated at 37 C for 4 h in DMEM supplemented with 0.5% BSA. Culture medium was collected and subjected to reverse-phase HPLC as described previously (6).

Small interfering RNA (siRNA)

Synthetic siRNAs and a negative control were purchased from Invitrogen (Carlsbad, CA). Two types of siRNAs specific for ghrelin *O*-acyltransferase (GOAT) were used: GCGCUUCUGUUUAAUUAUCUCUGCA (si1) and AGGAAGUCCAUAGGCUGACCUUCUU (si2). siRNAs were delivered into MGN3-1 cells using Lipofectamine RNAi Max (Invitrogen) according to the protocol provided by the manufacturer. The medium was changed after a 24-h incubation with siRNA. One mM of octanoic acid was added to the medium. Ghrelin levels in the media were measured after additional 6-d incubation.

Transplantation of MGN3-1 cells in nude mice

Eight-week-old male KSN nude mice were sc injected with 1.0×10^7 of MGN3-1 cells dissolved in PBS. Mice were housed individually with continuous access to chow and water. Food intake was measured by subtracting the remaining weight of the chow from that originally presented.

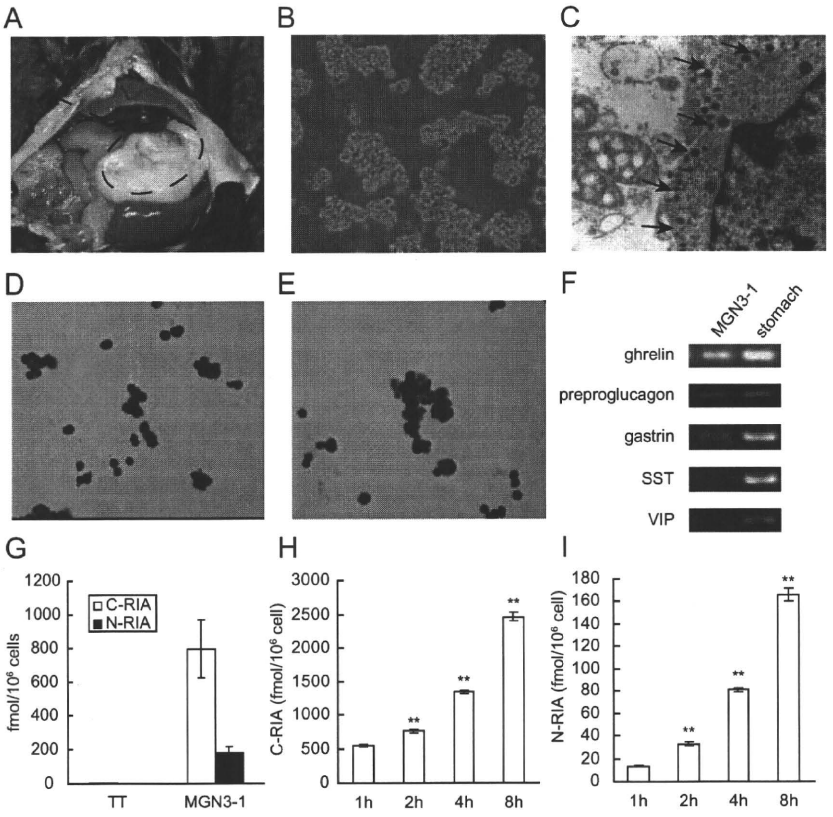

FIG. 1. Establishment of MGN3-1 cells A, Macroscopic findings of a ghrelinoma in a GP-Tag Tg mouse. B and C, Morphology of MGN3-1 cells by optic (B) and electron (C) microscopy. Secretory granules were observed (*arrow*). D and E, MGN3-1 cells were immunostained with anti-C-terminal ghrelin (D) and anti-N-terminal (E) ghrelin antibodies. F, RT-PCR analysis of the expression of mRNAs encoding gastric hormones in MGN3-1 cells. SST, Somatostatin; VIP, vasoactive intestinal polypeptide. G, Ghrelin peptide content determined by C-RIA and N-RIA in TT and MGN3-1 cells. H and I, Time course changes of ghrelin levels in the medium in which MGN3-1 cells were incubated. **, $P < 0.01$ compared with 1 h (n = 9).

Measurements of plasma ghrelin concentrations

Plasma samples were collected as reported previously (10). Plasma ghrelin and desacyl ghrelin concentrations were determined using an active ghrelin ELISA kit that recognizes *n*-octanoylated ghrelin and a desacyl ghrelin ELISA kit (both from Mitsubishi Kagaku Iatron, Tokyo, Japan), respectively (15).

Batch incubation study

MGN3-1 cells were seeded and cultured overnight in 12-well plates (7.5×10^5 cells/well). After a washing in PBS, cells were incubated at 37 C for 4 h in DMEM or Krebs-Ringer buffer (KRB) supplemented with 0.5% BSA and the indicated additional reagents (octanoic acid, somatostatin, or insulin) before collecting supernatants. Ghrelin concentrations in the supernatant were measured by RIA as described above. To determine the expression levels of ghrelin and GOAT mRNA, cells were incubated at 37 C for 24 h in DMEM supplemented with 0.5% BSA and the indicated additional reagents.

Statistical analysis

All values were expressed as the means ± SE. The statistical significance of the differences in mean values was assessed by ANOVA with a *post hoc* test (Tukey's test) or Student's *t* test as appropriate. Difference with $P < 0.05$ was considered significant.

Results

Establishment of MGN3-1 cell line

GP-Tag Tg mice (10) develop gastric tumors (Fig. 1A), which produce and secrete ghrelin and preserving the physiological regulation, at least by feeding status, sex difference, and body weights *in vivo*. We established a cell line, MGN3-1 cell, from a gastric tumor derived from a GP-Tag Tg mouse (Fig. 1A). MGN3-1 cells formed round-shaped aggregates that stuck together with moderate adhesion to culture dishes (Fig. 1B). These cells contained secretory granules when observed by electron microscopy (Fig. 1C). MGN3-1 cells exhibited ghrelin-like immunoreactivity by immunocytochemistry using anti-N-terminal, which recognizes ghrelin only, and anti-C-terminal ghrelin, which recognizes both ghrelin and desacyl ghrelin, antibodies (Fig. 1, D and E). We found the production of ghrelin mRNA by MGN3-1 cells using RT-PCR (Fig. 1F). This method also detected low levels of preproglucagon and gastrin mRNA (Fig. 1F) in MGN3-1 cells, whereas immunostaining with antiglucagon and antigastrin antibodies could not detect any expression of these proteins (data not shown). No expression of somatostatin and vasoactive intestinal polypeptide mRNA was observed in MGN3-1 cell (Fig. 1F). MGN3-1 cells contained approximately 140-fold higher levels of total ghrelin (*n*-octanoylated ghrelin plus desacyl ghrelin) measured by C-RIA and approximately 5000-fold higher levels of ghrelin measured by N-RIA than those observed in TT cells (Fig. 1G). The ghrelin levels in the medium were increased time dependently when MGN3-1 cells were incubated in DMEM (Fig. 1, H and I).

Acyl modification and maturation of ghrelin in MGN3-1 cells

MGN3-1 cells expressed GOAT, prohormone convertase (PC) 1/3 and PC2 mRNA (Fig. 2A). The molecular size of ghrelin examined by tricine SDS-PAGE and Western blot analysis in culture medium was consistent with that of mature ghrelin (Fig. 2B). In addition, when the culture

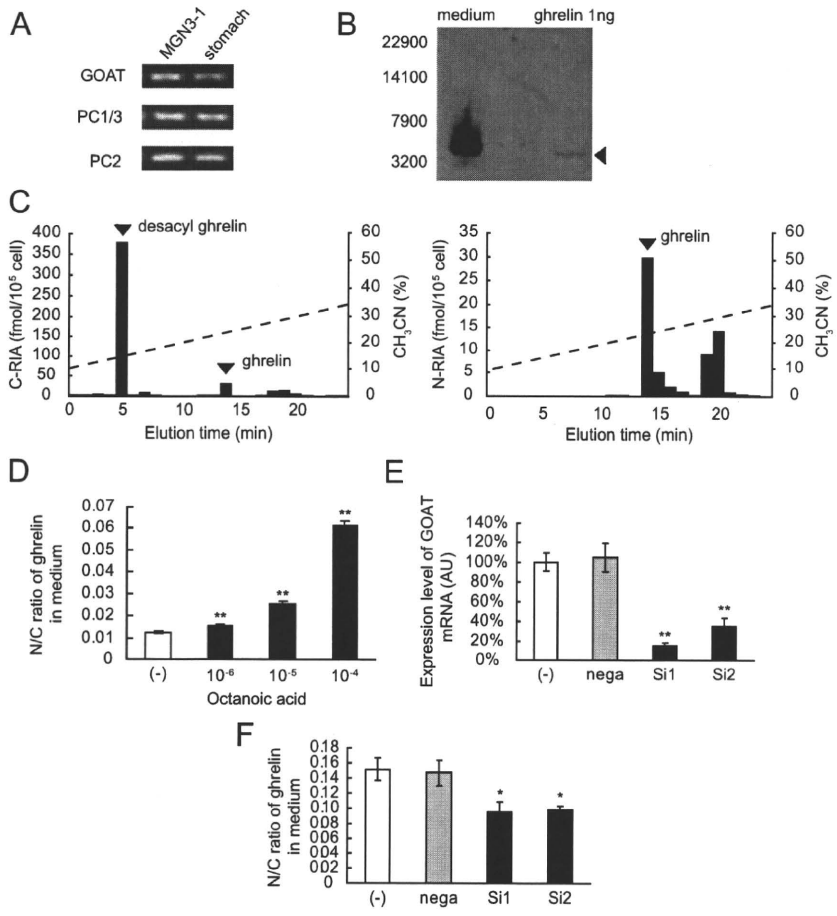

FIG. 2. Acylation and processing of ghrelin in MGN3-1 cells. A, RT-PCR analysis of GOAT, PC1/3, and PC2 mRNA expressions in MGN3-1 cells. B, Western blot analysis of culture medium in which MGN3-1 cells were cultured for 3 d. Rat ghrelin peptide was used as a positive control. C, Representative reverse-phase HPLC profiles of ghrelin immunoreactivity in the medium in which MGN3-1 cells were cultured for 4 h. D, The ratio of N-RIA to C-RIA of ghrelin secreted by MGN3-1 cells incubated for 4 h in KRB supplemented with 0.5% BSA and various concentrations of octanoic acid. **, $P < 0.01$ in comparison with (−) (n = 9). E, GOAT mRNA levels after siRNA treatment of MGN3-1 cells. Two types of siRNA specific for GOAT (Si1 and Si2) and negative control (nega) were introduced into MGN3-1 cell. *, $P < 0.05$, **, $P < 0.01$ in comparison with (−) (n = 7). AU, Arbitrary unit. F, The ratio of N-RIA to C-RIA of ghrelin secreted by MGN3-1 cells after siRNA treatment. *, $P < 0.05$, **, $P < 0.01$ in comparison with (−) (n = 7).

media were subjected to reverse-phase HPLC, the immunoreactive peaks detected by C-RIA and N-RIA were eluted at the positions identical with those of desacyl ghrelin and ghrelin (Fig. 2C). When MGN3-1 cells were incubated in KRB supplemented with 0.5% BSA, addition of octanoic acid to KRB significantly increased the ratio of *n*-octanoylated ghrelin measured by N-RIA to total ghrelin measured by C-RIA (N to C ratio) (Fig. 2D). Specific siRNA1 and siRNA2 treatment decreased GOAT mRNA levels in MGN3-1 cells to 85 and 65% of normal levels, respectively (Fig. 2E). The N to C ratio was significantly decreased by GOAT knockdown (Fig. 2F), indicating that GOAT mediates the acylation of ghrelin in MGN3-1 cells.

Transplantation of MGN3-1 cell to nude mouse

When MGN3-1 cells were injected sc into nude mice, they developed solid tumors (Fig. 3A). Plasma ghrelin and desacyl ghrelin levels were significantly elevated in nude mice 4 wk after MGN3-1 cell injection (Fig. 3, B and C). Mice injected with MGN3-1 cells exhibited significantly higher food intake in comparison with controls (PBS *vs.* cell: 21.4 ± 0.5 *vs.* 23.3 ± 0.7 g/wk, $P < 0.05$) 4 wk after injection (Fig. 3C).

The effect of somatostatin and insulin on ghrelin secretion and expression *in vitro*

MGN3-1 cells expressed the mRNAs encoding multiple somatostatin receptors, primarily type 2 and 5 with lower levels of type 3 and 4 (Fig. 4A. When somatostatin was added to culture media, ghrelin secretion was suppressed in a dose-dependent manner (Fig. 4, B and C). MGN3-1 cells also expressed mRNA of insulin receptor (Fig. 4A). Addition of insulin to culture media also suppressed ghrelin secretion from MGN3-1 cell (Fig. 4, D and E). Somatostatin treatment did not affect mRNA expression of either ghrelin or GOAT, even for 24 h incubation (Fig. 4, F and G), whereas insulin significantly suppressed them (Fig. 4, H and I).

Discussion

In this study, we successfully established the first ghrelinoma cell line, MGN3-1 cell. When establishing a cell line for a research tool, the most important thing is how the established cell line keeps its original characteristics. We evaluated the value of MGN3-1 cell by three points: the quantity of ghrelin production, the maintenance of machineries involved in acyl modification and maturation of ghrelin, and the preservation of known *in vivo* regulation of ghrelin secretion.

With regard to the amount of ghrelin production, MGN3-1 cells produced substantial quantities of ghrelin, approximately 5000-fold greater than that produced by

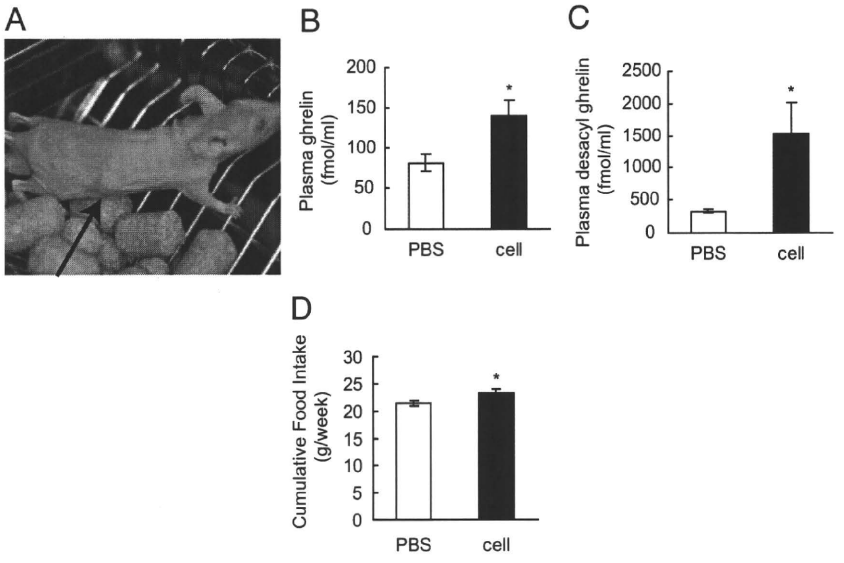

FIG. 3. Transplantation of MGN3-1 cell to nude mouse. A, Macroscopic findings of nude mice injected with MGN3-1 cells. B and C, Plasma ghrelin (B) and desacyl ghrelin (C) levels in nude mice at 4 wk after injection of saline or MGN3-1 cells. D, Cumulative food intake over a week (between 4 and 5 wk after injection) by mice injected with MGN3-1 cells (cell) or PBS. *, $P < 0.05$ in comparison with PBS (n = 5).

TT cells (6). It may be reasonable because TT cell is originated from thyroid medullary carcinoma, not from gastric ghrelin-producing cells. As for the machinery of ghrelin acyl modification and maturation, the MGN3-1 cell expressed two key enzymes: GOAT for acylation (16) and PC1/3 for processing (17). We confirmed the activity of GOAT in the MGN3-1 cell by the experiment in which the ratio of ghrelin to total ghrelin levels was decreased by knocking down the GOAT in MGN3-1 cells. Furthermore, addition of octanoic acid significantly increased the N to C ratio of ghrelin in the medium, which is consistent with the *in vivo* finding by Nishi *et al.* (18). We consider these findings important because acyl modification of ghrelin is one of the targets of drug discovery. On the other hand, tricine-SDS PAGE followed by Western blot analysis and reverse-phase HPLC confirmed the maturation of ghrelin in MGN3-1 cells. To provide a concrete evidence for the ability of producing bioactive ghrelin of MGN 3-1 cells, we performed a transplantation of MGN3-1 cells to nude mice, which resulted in the increase in plasma ghrelin levels and the enhancement of food intake in the nude mice. These results indicate that MGN3-1 cell keeps the ability to produce a substantial amount of bioactive ghrelin with normal acyl modification and maturation.

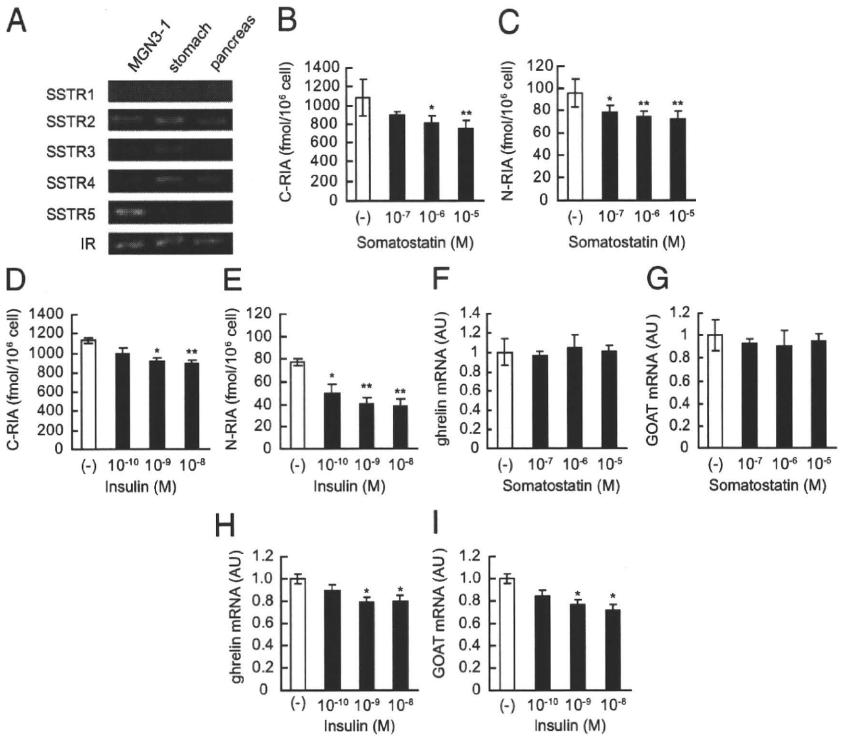

FIG. 4. The effect of somatostatin and insulin on ghrelin secretion and expression in MGN3-1 cells. A, RT-PCR analysis of somatostatin receptor (SSTR) types 1–5 and insulin receptor (IR) mRNA expressions in MGN3-1 cells. B–F, Ghrelin secretion was suppressed when MGN3-1 cells were incubated in DMEM supplemented with somatostatin (B and C) or insulin (D and E) for 4 h (n = 6). F–I, Somatostatin did not affect the expression levels of ghrelin (F) and GOAT (G) mRNA in MGN3-1 cell after 24 h incubation, whereas insulin significantly suppressed the expression levels of ghrelin (H) and GOAT (I) mRNA (n = 6). AU, Arbitrary unit. *, $P < 0.05$, **, $P < 0.01$ in comparison with (−).

Lastly, we examined the effect of a factor known to effect ghrelin secretion *in vivo*. Numerous reports exist examining the factors that regulate ghrelin secretion *in vivo* (19–27). Among those, the suppression of ghrelin secretion by somatostatin (19–22) or insulin (28, 29) is well established. We confirmed that ghrelin secretion is suppressed by somatostatin and insulin in MGN3-1 cells, indicating that MGN3-1 cells preserves the intrinsic characteristics of ghrelin-producing cells, at least with regard to its regulation by somatostatin and insulin.

In summary, we have established the first ghrelinoma cell line MGN3-1. The MGN3-1 cell line produces high amounts of bioactive ghrelin with normal acyl modification and maturation and retains physiological regulation by somatostatin. MGN3-1 will be a useful tool for

studying ghrelin production and secretion as well as for screening of ghrelin-modulating drugs.

Acknowledgments

We thank Ms. Chieko Ishimoto and Ms. Chinami Shiraiwa for their excellent technical assistance.

Address all correspondence and requests for reprints to: Hiroshi Iwakura, M.D., Ph.D., 54 Shogoin Kawahara-cho, Sakyo-ku, Kyoto 606-8507, Japan. E-mail: hiwaku@kuhp.kyoto-u.ac.jp.

This work was supported by funds from the Ministry of Education, Culture, Sports, Science, and Technology of Japan and the Ministry of Health, Labor, and Welfare of Japan.

Disclosure Summary: All authors have nothing to declare.

References

1. Kojima M, Hosoda H, Date Y, Nakazato M, Matsuo H, Kangawa K 1999 Ghrelin is a growth-hormone-releasing acylated peptide from stomach. Nature 402:656–660
2. Cummings DE, Purnell JQ, Frayo RS, Schmidova K, Wisse BE, Weigle DS 2001 A preprandial rise in plasma ghrelin levels suggests a role in meal initiation in humans. Diabetes 50:1714–1719
3. Tschöp M, Wawarta R, Riepl RL, Friedrich S, Bidlingmaier M, Landgraf R, Folwaczny C 2001 Post-prandial decrease of circulating human ghrelin levels. J Endocrinol Invest 24:RC19–RC21
4. Tschöp M, Weyer C, Tataranni PA, Devanarayan V, Ravussin E, Heiman ML 2001 Circulating ghrelin levels are decreased in human obesity. Diabetes 50:707–709
5. Ariyasu H, Takaya K, Tagami T, Ogawa Y, Hosoda K, Akamizu T, Suda M, Koh T, Natsui K, Toyooka S, Shirakami G, Usui T, Shimatsu A, Doi K, Hosoda H, Kojima M, Kangawa K, Nakao K 2001 Stomach is a major source of circulating ghrelin, and feeding state determines plasma ghrelin-like immunoreactivity levels in humans. J Clin Endocrinol Metab 86:4753–4758
6. Kanamoto N, Akamizu T, Hosoda H, Hataya Y, Ariyasu H, Takaya K, Hosoda K, Saijo M, Moriyama K, Shimatsu A, Kojima M, Kangawa K, Nakao K 2001 Substantial production of ghrelin by a human medullary thyroid carcinoma cell line. J Clin Endocrinol Metab 86:4984–4990
7. De Vriese C, Delporte C 2007 Autocrine proliferative effect of ghrelin on leukemic HL-60 and THP-1 cells. J Endocrinol 192:199–205
8. De Vriese C, Grégoire F, De Neef P, Robberecht P, Delporte C 2005 Ghrelin is produced by the human erythroleukemic HEL cell line and involved in an autocrine pathway leading to cell proliferation. Endocrinology 146:1514–1522
9. Gutierrez JA, Solenberg PJ, Perkins DR, Willency JA, Knierman MD, Jin Z, Witcher DR, Luo S, Onyia JE, Hale JE 2008 Ghrelin octanoylation mediated by an orphan lipid transferase. Proc Natl Acad Sci USA 105:6320–6325
10. Iwakura H, Ariyasu H, Li Y, Kanamoto N, Bando M, Yamada G, Hosoda H, Hosoda K, Shimatsu A, Nakao K, Kangawa K, Akamizu T 2009 A mouse model of ghrelinoma exhibited activated growth hormone-insulin-like growth factor I axis and glucose intolerance. Am J Physiol Endocrinol Metab 297:E802–E811
11. Iwakura H, Hosoda K, Doi R, Komoto I, Nishimura H, Son C, Fujikura J, Tomita T, Takaya K, Ogawa Y, Hayashi T, Inoue G, Akamizu T, Hosoda H, Kojima M, Kangawa K, Imamura M, Nakao K 2002 Ghrelin expression in islet cell tumors: augmented expression of ghrelin in a case of glucagonoma with multiple endocrine neoplasm type I. J Clin Endocrinol Metab 87:4885–4888
12. Hosoda H, Kojima M, Matsuo H, Kangawa K 2000 Ghrelin and des-acyl ghrelin: two major forms of rat ghrelin peptide in gastrointestinal tissue. Biochem Biophys Res Commun 279:909–913
13. Iwakura H, Ariyasu H, Kanamoto N, Hosoda K, Nakao K, Kangawa K, Akamizu T 2008 Establishment of a novel neuroblastoma mouse model. Int J Oncol 33:1195–1199
14. Iwakura H, Hosoda K, Son C, Fujikura J, Tomita T, Noguchi M, Ariyasu H, Takaya K, Masuzaki H, Ogawa Y, Hayashi T, Inoue G, Akamizu T, Hosoda H, Kojima M, Itoh H, Toyokuni S, Kangawa K, Nakao K 2005 Analysis of rat insulin II promoter-ghrelin transgenic mice and rat glucagon promoter-ghrelin transgenic mice. J Biol Chem 280:15247–15256
15. Akamizu T, Shinomiya T, Irako T, Fukunaga M, Nakai Y, Kangawa K 2005 Separate measurement of plasma levels of acylated and desacyl ghrelin in healthy subjects using a new direct ELISA. J Clin Endocrinol Metab 90:6–9
16. Yang J, Brown MS, Liang G, Grishin NV, Goldstein JL 2008 Identification of the acyltransferase that octanoylates ghrelin, an appetite-stimulating peptide hormone. Cell 132:387–396
17. Zhu X, Cao Y, Voogd K, Voogd K, Steiner DF 2006 On the processing of proghrelin to ghrelin. J Biol Chem 281:38867–38870
18. Nishi Y, Hiejima H, Hosoda H, Kaiya H, Mori K, Fukue Y, Yanase T, Nawata H, Kangawa K, Kojima M 2005 Ingested medium-chain fatty acids are directly utilized for the acyl modification of ghrelin. Endocrinology 146:2255–2264
19. Shimada M, Date Y, Mondal MS, Toshinai K, Shimbara T, Fukunaga K, Murakami N, Miyazato M, Kangawa K, Yoshimatsu H, Matsuo H, Nakazato M 2003 Somatostatin suppresses ghrelin secretion from the rat stomach. Biochem Biophys Res Commun 302:520–525
20. Silva AP, Bethmann K, Raulf F, Schmid HA 2005 Regulation of ghrelin secretion by somatostatin analogs in rats. Eur J Endocrinol 152:887–894
21. Norrelund H, Hansen TK, Orskov H, Hosoda H, Kojima M, Kangawa K, Weeke J, Moller N, Christiansen JS, Jorgensen JO 2002 Ghrelin immunoreactivity in human plasma is suppressed by somatostatin. Clin Endocrinol (Oxf) 57:539–546
22. Broglio F, Koetsveld Pv P, Benso A, Gottero C, Prodam F, Papotti M, Muccioli G, Gauna C, Hofland L, Deghenghi R, Arvat E, Van Der Lely AJ, Ghigo E 2002 Ghrelin secretion is inhibited by either somatostatin or cortistatin in humans. J Clin Endocrinol Metab 87:4829–4832
23. Sugino T, Yamaura J, Yamagishi M, Kurose Y, Kojima M, Kangawa K, Hasegawa Y, Terashima Y 2003 Involvement of cholinergic neurons in the regulation of the ghrelin secretory response to feeding in sheep. Biochem Biophys Res Commun 304:308–312
24. Broglio F, Gottero C, Van Koetsveld P, Prodam F, Destefanis S, Benso A, Gauna C, Hofland L, Arvat E, van der Lely AJ, Ghigo E 2004 Acetylcholine regulates ghrelin secretion in humans. J Clin Endocrinol Metab 89:2429–2433
25. Grinspoon S, Miller KK, Herzog DB, Grieco KA, Klibanski A 2004 Effects of estrogen and recombinant human insulin-like growth factor-I on ghrelin secretion in severe undernutrition. J Clin Endocrinol Metab 89:3988–3993
26. Koutkia P, Canavan B, Breu J, Johnson ML, Grinspoon SK 2004 Nocturnal ghrelin pulsatility and response to growth hormone secretagogues in healthy men. Am J Physiol Endocrinol Metab 287: E506–E512
27. Basa NR, Wang L, Arteaga JR, Heber D, Livingston EH, Taché Y 2003 Bacterial lipopolysaccharide shifts fasted plasma ghrelin to postprandial levels in rats. Neurosci Lett 343:25–28
28. Murdolo G, Lucidi P, Di Loreto C, Parlanti N, De Cicco A, Fatone C, Fanelli CG, Bolli GB, Santeusanio F, De Feo P 2003 Insulin is required for prandial ghrelin suppression in humans. Diabetes 52:2923–2927
29. Saad MF, Bernaba B, Hwu CM, Jinagouda S, Fahmi S, Kogosov E, Boyadjian R 2002 Insulin regulates plasma ghrelin concentration. J Clin Endocrinol Metab 87:3997–4000

Generation of Transgenic Mice Overexpressing a Ghrelin Analog

Go Yamada, Hiroyuki Ariyasu, Hiroshi Iwakura, Hiroshi Hosoda, Takashi Akamizu, Kazuwa Nakao, and Kenji Kangawa

Department of Endocrinology and Metabolism (G.Y., K.N.), Kyoto University Graduate School of Medicine, and Ghrelin Research Project (H.A., H.I., T.A., K.K.), Translational Research Center, Kyoto University Hospital, Kyoto 606-8507, Japan; and Department of Biochemistry (H.H., K.K.), National Cardiovascular Center Research Institute, Osaka 565-8565, Japan

After the discovery of ghrelin, we attempted to generate ghrelin gene transgenic (Tg) mice. These animals, however, produced only des-acyl ghrelin, which lacked the n-octanoyl modification at Ser^3 necessary to manifest ghrelin activity. Because the mechanism for acyl-modification of ghrelin had been unclear until the recent identification of GOAT (ghrelin O-acyltransferase), it had been difficult to generate Tg mice overexpressing ghrelin using standard procedures. Therefore, we planned to generate Tg mice overexpressing a ghrelin analog, which possessed ghrelin-like activity in the absence of acylation at Ser^3 and could be synthesized *in vivo*. As the replacement of Ser^3 of ghrelin with Trp^3 (Trp^3-ghrelin) preserves a low level of ghrelin activity and Trp^3-ghrelin can be synthesized *in vivo*, we generated mice overexpressing Trp^3-ghrelin by using the hSAP (human serum-amyloid-P) promoter. Plasma Trp^3-ghrelin concentrations in the Tg mice were approximately 85-fold higher than plasma ghrelin concentrations in non-Tg littermates. Because Trp^3-ghrelin is approximately 1/10–1/20 less potent than ghrelin *in vivo*, plasma Trp^3-ghrelin concentrations in Tg mice were calculated to have an activity approximately 6-fold greater than that of acylated ghrelin seen in non-Tg mice (85-fold x 1/10–1/20). Tg mice exhibited a normal growth and glucose metabolism in their early life stage. However, 1-yr-old Tg mice demonstrated impaired glucose tolerance and reduced insulin sensitivity. This model will be useful to evaluate the long-term effects of ghrelin or ghrelin analogs. In addition, this technique may be a useful method to generate gain-of-activity models for hormones that require posttranscriptional modifications. (***Endocrinology*** **151: 5935–5940, 2010)**

Ghrelin, an endogenous ligand for the GH secretagogue receptor (GHS-R) (or ghrelin receptor), is a stomach-derived 28-amino acid peptide hormone modified by n-ontanoylic acid at the third Ser residue (Ser^3) (1). This modification is essential for ghrelin activity (1).

Since ghrelin was discovered, several groups, including us, have been trying to generate transgenic (Tg) mice overexpressing ghrelin under the control of different promoters (2–7). All of these animals, with the exception of two lines created by Reed *et al.* (5) and Bewick *et al.* (8), produced des-acyl ghrelin only. This form lacks the n-octanoyl modification at Ser^3 and is devoid of ghrelin activity. The mechanism for ghrelin acylation had been unclear until the recent identification of ghrelin O-acyltransferase (GOAT) (9). Because GOAT had not yet been identified when we initiated this study and it had proved to be difficult to generate the Tg mice overexpressing ghrelin by standard procedures, we planned to generate Tg mice overexpressing a ghrelin analog possessing ghrelin-like activity without Ser^3 acylation that could be synthesized *in vivo*.

Matsumoto *et al.* (10) investigated the effect on ghrelin bioactivities of replacement of the octanoylated Ser at the third position with other amino acids, such as tryptophan

ISSN Print 0013-7227 ISSN Online 1945-7170
Printed in U.S.A.

doi: 10.1210/en.2010-0635 Received June 4, 2010. Accepted September 20, 2010.
First Published Online October 20, 2010

Abbreviations: C-RIA, RIA recognizing the C-terminal region of ghrelin; GOAT, ghrelin O-acyltransferase; GHS-R, GH secretagogue receptor; hSAP, human serum-amyloid-P; N-RIA, RIA recognizing the N-terminal region of ghrelin; Tg, transgenic; Trp, tryptophan; Trp^3-ghrelin, ghrelin analog with the third amino-acid residue (Ser^3) replaced by Trp.

(Trp), Val, Leu, or Ile. The ghrelin-like activity of these synthetic peptides was evaluated by EC_{50} values, determined by an increase in intracellular calcium concentrations $[Ca^{2+}]_i$ in GHS-R-expressing cells. Replacement of Ser^3 with Trp^3 (Trp^3-ghrelin) preserved ghrelin activity with an EC_{50} of 31 nM in comparison with 1.3 nM for intact ghrelin. Replacement of Ser^3 with Val^3, Leu^3, or Ile^3 led to complete loss of ghrelin potency. Although ghrelin analog, in which the Ser^3 residue was replaced by Trp (Trp^3-ghrelin) is approximately 24-fold less active than native ghrelin *in vitro*, it can be synthesized *in vivo*. Thus, we selected Trp^3-ghrelin as a candidate ghrelin analog.

In this study, we examined whether Trp^3-ghrelin exerts ghrelin-like activity *in vivo*. After confirming this activity, we generated Tg mice overexpressing Trp^3-ghrelin.

Materials and Methods

All animal protocols were approved by the Kyoto University Graduate School of Medicine Committee on Animal Research. Animals, housed in air-conditioned animal quarters with light between 0800 and 2000 h, were maintained on standard rat chow (CE-2, 352 kcal/100 g; Japan CLEA, Osaka, Japan).

Experiment 1, the *in vivo* effects of Trp^3-ghrelin

Eight-week-old male C57BL/6 mice were purchased from Japan CLEA. Ghrelin was obtained from Peptide Research Institute (Osaka, Japan). Trp^3-ghrelin, in which the Ser^3 residue was replaced by Trp, was synthesized as previously described (10).

Food intake

Mice (n = 8, each group) were injected sc with saline, ghrelin (120 or 360 mcg/kg), or Trp^3-ghrelin (360, 1200, or 3600 mcg/kg) before measuring a 2-h food intake.

GH secretion

Mice (n = 8, each group) were injected with iv saline, ghrelin (4, 12, 40, or 120 mcg/kg), or Trp^3-ghrelin (12, 40, 120, or 360 mcg/kg). Blood samples were collected from the retro-orbital vein 10 min after injection and stored at −20 C until assessed.

Inhibition of glucose stimulated insulin secretion

After a 12-h fast, mice (n = 8, each group) were injected iv with 1.0 g/kg glucose, together with saline, ghrelin (120 or 360 mcg/kg), or Trp^3-ghrelin (1200 or 3600 mcg/kg). Blood samples were collected 1 and 10 min after injection and stored at −20 C until assessed.

Experiment 2, generation of Tg mice overexpressing a ghrelin analog, Trp^3-ghrelin

Plasmid construction and generation of Tg mice

We generated a fusion gene of the human serum-amyloid-P (hSAP) promoter and full-length mouse preproghrelin cDNA (1, 11). Plasmid hSAP-ghrelin was constructed by inserting mouse preproghrelin cDNA into the unique *Eco*RI site between the hSAP promoter and the 3′-flanking sequence of the rabbit β-globin gene. Mutations were created using a QuikChange Site-Directed Mutagenesis kit, according to the manufacturer's instruction. The hSAP-ghrelin plasmid was used as the template for PCR amplification. To replace the AGC codon encoding Ser to a TGG codon encoding Trp, we used two oligonucleotide primers: 5′-GGACATGGCCATGGCAGGCTCCTGGTTCCTGAGCCCAGAGC-3′ and 5′-GCTCTGGGCTCAGGAACCAGGAGCCTGCCATGGCCATGTCC-3′. The mutated construct was verified by sequencing (please see figure 2A). The DNA fragment encoding mutant ghrelin was excised from the plasmid by digestion with *Sal*I and *Hin*dIII (see figure 2B), then purified and microinjected into the pronuclei of fertilized eggs as reported (11). Founder Tg mice were identified by PCR analysis and bred against C57BL/6 mice.

Please refer to Supplemental Methods, published on The Endocrine Society's Journals Online web site at http://endo.endojournals.org, for real-time quantitative RT-PCR, semiquantitative PCR, glucose and insulin tolerance tests, measurements of insulin-releasing ability, body weights, body length, body composition, daily food intake, hormonal parameters, and statistical analyses.

Results

Experiment 1, the *in vivo* effects of Trp^3-ghrelin on food intake and GH secretion

To elucidate whether Trp^3-ghrelin has ghrelin-like potency *in vivo*, 8-wk-old male C57BL/6 mice were administrated vehicle, ghrelin, or Trp^3-ghrelin before determining food intake over a period of 2 h. Injection of ghrelin or Trp^3-ghrelin stimulated food intake in a dose-dependent manner (Fig. 1A). The 2-h food intake after injection of 3600 mcg/kg of Trp^3-ghrelin was 0.47 ± 0.04 g, which was 2.2-fold higher than that seen in vehicle-injected mice (0.21 ± 0.02 g/2 h). This level of stimulation was similar to that seen in mice injected with ghrelin at a dose of 360 mcg/kg. Serum GH levels increased after injection of 360 mcg/kg Trp^3-ghrelin to 133.9 ± 46.1 ng/ml, which was 21-fold higher than that seen after vehicle injection (6.4 ± 1.1 ng/ml) and similar to those seen after ghrelin injection at 40 mcg/kg (138.8 ± 26.5 ng/ml, respectively) (Fig. 1B). Injection of ghrelin or Trp^3-ghrelin inhibited glucose-stimulated insuline release in a dose-dependent manner (Fig. 1C). The 10-min insulin response was significantly inhibited by 3600 mcg/kg Trp^3-ghrelin and 360 mcg/kg to the same extent (0.78 ± 0.09 and 0.63 ± 0.06 ng/ml), compared with saline (1.10 ± 0.01 ng/ml). These results indicated that Trp^3-ghrelin stimulates food intake and GH secretion and inhibits glucose-stimulated insulin secretion in a manner similar to ghrelin with a potency approximately 1/10–1/20 (Trp^3-ghrelin needs about 20-fold amount for stimulation of food intake, about 10-fold amount for GH secretion, and about 10-fold amount for